

**ROLE OF ING2 (INHIBITOR OF GROWTH FAMILY MEMBER 2) IN CELLULAR
RESPONSES TO DNA DAMAGE**

by

Guoming Sun

Bachelor of Science, Peking University, 2001

Submitted to the Graduate Faculty of
The School of Medicine in partial fulfillment
of the requirements for the degree of
Doctor of Philosophy

University of Pittsburgh

2009

UNIVERSITY OF PITTSBURGH

SCHOOL OF MEDICINE

This dissertation was presented

by

Guoming Sun

It was defended on

[January 16th, 2009]

and approved by

Dr. Baskaran Rajasekaran, Ph.D.
Associate Professor
Dept. of Microbiology & Molecular Genetics
Dissertation Advisor

Dr. Shi-Yuan Cheng, Ph.D.
Associate Professor
Dept. of Pathology
Committee Member

Dr. Saleem Khan, Ph.D.
Professor
Dept. of Microbiology & Molecular Genetics
Committee Member

Dr. Martin Schmidt, Ph.D.
Associate Professor
Dept. of Microbiology & Molecular Genetics
Committee Member

Dr. Lin Zhang, Ph.D.
Associate Professor
Dept. of Pharmacology & Chemical Biology
Committee Member

Copyright © by Guoming Sun

2009

ROLE OF ING2 (INHIBITOR OF GROWTH FAMILY MEMBER 2) IN CELLULAR RESPONSES TO DNA DAMAGE

Guoming Sun, Ph.D.

University of Pittsburgh, 2009

Genome stability is essential for cells to survive. Consequently, cells have evolved intricate responses that include transcriptional changes, cell-cycle arrest, activation of DNA repair, and apoptosis. Such responses prevent permanent fixation of DNA damage induced by genotoxic agents into the genome, thus contributing to genome stability.

A collection of proteins implicated in DNA damage responses are called Inhibition of Growth (ING) family, which are a group of small molecular weight proteins that regulate a variety of biological functions ranging from senescence, cell cycle arrest, apoptosis and DNA repair. ING proteins interact with Histone Acetyl-transferases (HAT) and Histone Deacetylases (HDAC) to alter the state of chromatin compaction and acetylation status of many proteins during DNA damage. A specific member of the ING family, ING2 has been implicated in modulating the tumor suppressor, p53 function through p300 HAT-mediated acetylation. Irradiation fails to upregulate ING2, but increases its association with transcription co-activator p300. That p300 HAT activation in the cells with ING2 knock down is hampered post-irradiation suggests that the interaction between ING2 and p300 is indispensable for the upregulation of the p300 HAT activity. Cells deficient in protein kinase Ataxia Telangiectasia Mutated (ATM) displays impaired p300 HAT activation and less association between p300 and ING2 following ionizing radiation, indicating that ATM function is also required.

Alkylating agent, *N*-methyl-*N'*-nitro-*N*-nitrosoguanidine (MNNG) upregulates ING2 level in both time- and dose-dependent manner. We further observed that ING2 regulates the cell

death response induced by this alkylator through a mechanism involving acetylation and stabilization of p73. Induction/acetylation of p53, in response to MNNG, however, proceeds in an ING2-independent manner. Inhibition of c-Abl by STI571 treatment blocked ING2 upregulation and p73 acetylation induced by MNNG. Similarly, MLH1- suppressed or mutated cells displayed defective ING2 upregulation and p73 acetylation in response to MNNG, which suggests that Mlh1- and c-Abl-dependent upregulation of ING2 activates the cell death response to MNNG through p73 acetylation.

Taken together, these findings demonstrate that ING2 plays an important role in the cellular responses to different DNA damage by regulating the acetylation of tumor suppressors.

TABLE OF CONTENTS

ACKNOWLEDGMENTS	XIII
1.0 INTRODUCTION.....	1
1.1 DNA DAMAGE	1
1.2 ING FAMILY AND ACETYLATION	2
2.0 ATM UP REGULATES P300 HAT ACTIVIT Y AFT ER IRRADI ATION THROUGH ING2	5
2.1 INTRODUCTION	6
2.1.1 Ataxia-Telangiectasia Mutated (ATM) and Double Stand Break (DSB)	6
2.1.2 p53 acetylation.....	8
2.1.3 Acetyltransferase.....	9
2.1.4 Summary.....	9
2.2 MATERIALS AND METHODS.....	10
2.2.1 Cell Culture	10
2.2.2 Irradiation	11
2.2.3 Reagents and Antibodies	11
2.2.4 Reversible cell permebilization	12
2.2.5 Immunoblotting.....	12
2.2.6 Immunoprecipitation	13

2.2.7	Histone Acetyltransferase (HAT) Assay	13
2.2.8	<i>In vitro</i> ATM Kinase Assay	14
2.2.9	RNA interference	15
2.2.10	Microscopy	15
2.3	RESULTS	16
2.3.1	IR induces p300 histone acetyltransferase activity.	16
2.3.2	IR-induced p300 HAT activation is not cell-line specific.	19
2.3.3	ATM is required for IR-induced p300 HAT activity upregulation.	19
2.3.4	Acetylation of p53 after IR is an ATM-dependent process.	22
2.3.5	Phospho- p53 is a preferred target for p300.	25
2.3.6	IR-induced acetylation of p53 is regulated by two converse mechanisms.	29
2.3.7	Relocalization of ING2 following γ-irradiation	31
2.3.8	ING2 is required for the IR-induced p53 acetylation.	34
2.3.9	p300 interacts with ING2 in an ATM-dependent manner.	36
2.4	DISCUSSION	38
2.4.1	p300 activation and phosphorylation	38
2.4.2	Role of ING2 in p300 HAT activation	39
2.4.3	Functional Relevance of Plant Homeodomain (PHD) in ING2	40
2.4.4	Functional role of p300 activation induced by IR in DNA repair	42
2.4.5	Functional Role of p300 activation induced by IR in apoptosis	43
2.5	SUMMARY	44

3.0	ING2 REGULATES MNNG-INDUCED APOPTOSIS THROUGH MMR/C-ABL-DEPENDENT P73 ACETYLATION	45
3.1	INTRODUCTION	46
3.1.1	Alkylating Agent: MNNG	46
3.1.2	Mismatch Repair System	46
3.1.3	Summary.....	48
3.2	MATERIALS AND METHODS	49
3.2.1	Materials	49
3.2.2	Cell lines.....	49
3.2.3	RNA interference	50
3.2.4	Immunoblotting.....	50
3.2.5	Immunoprecipitation	50
3.2.6	Transfection.....	51
3.2.7	Flow cytometry.....	51
3.3	RESULTS	53
3.3.1	Dose- and time-dependent Induction of ING2 in response to MNNG treatment.....	53
3.3.2	ING2 is required for MNNG-induced cell death	55
3.3.3	ING2 is dispensable for p53 stabilization/acetylation induced by MNNG	57
3.3.4	ING2 regulates p73 induction/acetylation in response to MNNG	59
3.3.5	p73 is required for MNNG-induced cell death.....	61

3.3.6	C-Abl-dependent acetylation of p73 activates the cell death response to MNNG.....	63
3.3.7	MMR dependency of ING2/ p73 induction by MNNG.....	65
3.3.8	ATM/ATR independency of ING2/ p 73 acetylation induction by MN NG	67
3.4	DISCUSSION.....	69
3.4.1	ING2 induction and c-Abl activation	69
3.4.2	p73 and MNNG-induced apoptosis	70
3.5	SUMMARY	73
4.0	SUMMARY & FUTURE DIRECTIONS	74
4.1	SUMMARY	74
4.2	FUTURE DIRECTIONS.....	76
4.2.1	Mapping of ATM phosphorylation site using MALDI-TOF Mass Spectrometry	76
4.2.2	Mechanism of ING2-mediated activation of p300	78
4.2.3	Role of ING2 relocation in p300 HAT activation.....	79
4.2.4	ING2 induction in response to MNNG	79
4.2.5	Role of MMR in MNNG-induced ING2 expression.....	80
4.2.6	ING2, p300 HAT activation and p73 acetylation in response to MNNG	80
	APPENDIX A. ACKNOWLEDGEMENTS.....	82
	APPENDIX B. PUBLICATIONS.....	83
	BIBLIOGRAPHY.....	84

LIST OF TABLES

Table 1: Candidate ATM target sequences in p300.....	77
--	----

LIST OF FIGURES

Figure 1: Structure of ING family proteins.....	4
Figure 2: Time and dose-dependent activation of p300 HAT activity by IR.	17
Figure 3: Time and dose-dependent p300 HAT activation in HEK-293, HeLa and MCF-7 cells following IR exposure.....	18
Figure 4: p300 HAT activation in the presence or absence of caffeine post-IR.....	20
Figure 5: IR-induced p300 HAT activation requires ATM.	21
Figure 6: Time-course of p53 acetylation and phosphorylation in 293 cells after IR	23
Figure 7: p53 acetylation after IR exposure is an ATM-dependent process.....	24
Figure 8: Phosphorylated p53 is a preferred substrate for acetylation.....	27
Figure 9: Increased p53 level is unable to upregulate p53 acetylation and phosphorylation without IR.	28
Figure 10: Effect of Lys-CoA and TSA on p53 phosphorylation and acetylation.	30
Figure 11: Relocalization of ING2 after IR.....	33
Figure 12: ING2 is indispensable for p53 acetylation induced by IR.....	35
Figure 13: Association between ING2 and p300 post –IR requires ATM function.	37
Figure 14: Proposed model for p300 HAT activation by ING2.	41
Figure 15: MNNG treatment induces ING2 in a time- and dose-dependent manner.	54

Figure 16: ING2 is required for MNNG-induced p73-mediated cell death.....	56
Figure 17: ING2 is dispensable for MNNG-induced p53 stabilization.	58
Figure 18: ING2 is required for MNNG-induced p73 acetylation.	60
Figure 19: MNNG-induced cell death in cells knocked down for ING2, p73 or both.	62
Figure 20: STI571 blocks MNNG-induced ING2 upregulation and p73 acetylation.....	64
Figure 21: MMR function is required for MNNG-induced ING2 induction and p73 acetylation.	66
Figure 22: ATM and ATR are dispensable for MNNG-induced ING2 induction.....	68
Figure 23: Proposed model for MMR-dependent activation of cell death by ING2.	72

ACKNOWLEDGMENTS

This work would have never been done without the help from many individuals. First of all, I would like to thank my advisor Dr. Baskaran Rajasekaran for his invaluable mentorship and support on this 4-year journey. Not only did he provide me the precious opportunity to explore the world of DNA damage, he also guided me through the various difficulties I met with his patience, enthusiasm and wisdom.

I am also greatly thankful to my doctoral dissertation committee members: Dr. Shi-Yuan Cheng, Dr. Saleem Khan, Dr. Martin Schmidt, and Dr. Lin Zhang for their tremendous help, time and expertise.

I would like to express my sincere gratitude to all the members of the Rajasekaran lab throughout the years. In particular I would like to thank Dr. Zhihua Jiang, Dr. Ravindra Kamath and Dr. Yajuan Gao. Their dedications to science and team work spirit create a conducive environment for me to do search, to communicate and to develop friendship. I am honored to work with them.

My sincere thanks also go to the current and previous members of the Graduate Office, especially Dr. Stephen Phillips, Cindy Duffy, Carol Staley, Jennifer Walker, Veronica Cardamone and Sandra Honick. They are so supportive during my graduate studies in the Interdisciplinary Biomedical Graduate Program at the University of Pittsburgh, School of Medicine.

I am indebted to staffs of the Department of Microbiology and Molecular Genetics, Roberta Cheplic, Dee O'Hara, Mary Ann Merranko, Joe Llana, Tim Reardon, Mary Beth Bowler and Diane Vaughan. They are always there when I need their help.

I have been blessed to have many wonderful friends. I could not imagine what my life would become without their support and encouragement. The joyful memories of the five years in Pittsburgh will be a life-time treasure to me.

I would like to thank my Chinese compatriots and our great motherland, China. This thesis would not have been possible without the path of reform and opening-up China embarked on 30 years ago.

Lastly, I wish to extend my sincere gratitude to my family, especially my parents. Their unreserved love is my everlasting source of faith, courage, strength and happiness. Since my childhood, they have been supporting my dream to be a Ph.D., which finally comes true today.

I cannot thank all these persons enough.

1.0 INTRODUCTION

1.1 DNA DAMAGE

Mutation in DNA occurs at a rate of 1,000 to 1,000,000 lesions per cell per day. Failure to repair the damaged DNA will result in mutations in the genome, thus loss of the integrity of the genetic information. The correctness of the genetic information is vital to keep the cells from malignancy or death (Browner *et al.*, 2004). To prevent permanent fixation of mutations, eukaryotic cells activate a complex signaling network that functions to mediate DNA repair and activate cell-cycle checkpoints. Persistent DNA damage activates cell death responses.

DNA damage can be classified into endogenous and exogenous damage. The endogenous damage can be induced by the normal metabolic byproducts, such as Reactive Oxygen Species (ROS) (Stadtman, 1992), and errors that occur during replication. Endogenous damage can further be subdivided into four major types according the modification inflicted on the DNA: oxidation, alkylation, hydrolysis and mismatch.

The exogenous DNA damage can be inflicted by multiple types of agents. For example, pyrimidine dimers introduced by UV, induces the cross linking between neighboring cytosine and thymine bases. Double Strand Breaks (DSBs) and Single Strand Breaks (SSDs) can be created by the ionizing radiation (IR) or high temperature, which are lethal to the cell. DNA

adducts can also be caused by mutagens such as polycyclic hydrocarbon or hydrogen peroxide (H₂O₂) originating from pollutants (Cadet *et al.*, 2008).

In general, damage such as thymine dimer induced by UV and methylation of DNA base introduced by chemicals can be corrected by direct reversal. In most cases, cells use the other strand as a template to correct the defect. Briefly, cells excise the defected strand, remove the impaired nucleotide and synthesize a new nucleotide to replace the defected one with the guidance of undamaged strand (Lindahl and Wood, 1999). Base Excision Repair (BER), Nucleotide Excision Repair (NER), and Mismatch Repair (MMR) are the three major excision repair mechanisms. To repair the especially hazardous double strand breaks, cells have evolved two mechanisms with different repair strategies, Non-Homologous End Joining (NHEJ) and Homologous Recombination (HR) (Moore and Haber, 1996). In NHEJ, two ends are joined directly by the DNA ligase IV without template guidance. NHEJ is a low-fidelity repair mechanism because of mutation, deletion or translocation incurred during the repair process (Budman and Chu, 2005). On the other hand, HR uses a sister chromatid or homologous chromosome as template to repair the break thus achieving high fidelity (Jung and Alt, 2004).

1.2 ING FAMILY AND ACETYLATION

Inhibitor of Growth (ING) family of proteins are a group of tumor suppressors that control cell growth/proliferation, and cancer (Campos *et al.*, 2004). All of the family members share a highly conserved Plant Homeodomain (PHD) near the C-terminal end and a nuclear localization sequence (NLS), as shown in Figure 1 (Gong *et al.*, 2005). The highly conserved structure of ING family suggests that they have similar functions in cells.

In *S. cerevisiae*, three ING proteins, namely Pho23, Yng1, and Yng2, co-purified as stable components of the Sin3/Rpd3 HDAC, NuA3, and NuA4 HAT complexes, respectively (Howe *et al.*, 2002; Nourani *et al.*, 2001; Nourani *et al.*, 2003). In higher organisms, ING1 is observed to reside within the mSin3A-HDAC complex (Kuzmichev *et al.*, 2002) and can also associate with the p300 HAT (Vieyra *et al.*, 2002). Similarly, ING3 is documented to form a stable complex with Tip60/NuA4 HAT (Doyon *et al.*, 2004). ING4 and ING5 have been found to associate with HBO1 HAT complex (Doyon *et al.*, 2006). Biochemical analysis showed that ING4 is essential for bulk histone H4 acetylation. All members of the ING family harbor a highly conserved Plant Homeodomain (PHD) that is commonly found in various chromatin remodeling proteins (Aasland *et al.*, 1995). The PHD of ING2 regulates p53-dependent apoptosis through phosphoinositides signaling (Gozani *et al.*, 2003). Genetic and crystal structure analyses revealed that ING proteins bind to trimethylated lysine of histone H3 in yeast and mammalian cells *via* the PHD finger (Martin *et al.*, 2006; Pena *et al.*, 2006; Shi *et al.*, 2006). There is some evidence that ING proteins may bind directly to DNA (Kataoka *et al.*, 2003). Deletion leucine zipper (LZL) domain in ING2 abrogated its association with p53, but not with p300. Conceivably, ING2 modulates p53-dependent chromatin remodeling, apoptosis and DNA repair by functioning as a scaffold protein to mediate the interaction between p53 and p300 (Wang *et al.*, 2006a; Wang *et al.*, 2006b).

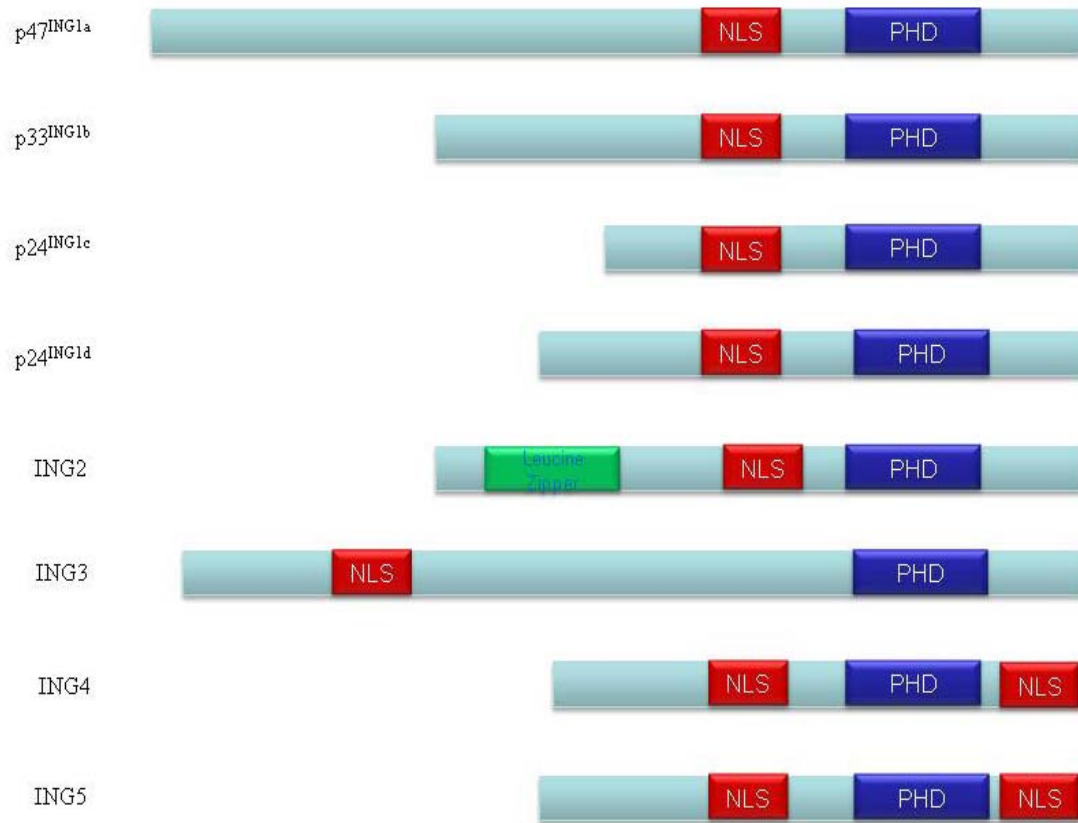


Figure 1: Structure of ING family proteins

PHD Plant Homeodomain

NLS Nuclear Localization Sequence

Leucine Zipper Leucine Zipper Domain

**2.0 ATM UPREGULATES P300 HAT ACTIVITY AFTER IRRADIATION
THROUGH ING2**

2.1 INTRODUCTION

2.1.1 Ataxia-Telangiectasia Mutated (ATM) and Double Stand Break (DSB)

DNA repair mechanisms are vital to the survival and normal functioning of the cells. Mutations or deletions in the regions encoding proteins composing these DNA repair machineries impair the mechanisms and result in loss of genome integrity. The failure of a mechanism to repair damaged DNA may lead cells to neoplasia and dysfunction. Several diseases linked to genetic defect disrupting these mechanisms are characterized by tissue degeneration (especially central nervous system and immune system), sensitivity to DNA damaging agents and high predisposition to cancer (Vessey *et al.*, 1999). One of these syndromes, Ataxia Telangiectasia (A-T), is a recessive autosomal human disorder. A-T patients show ocular telangiectasia, progressive neuronal degeneration, immune deficiency, extreme sensitivity to ionizing radiation, premature aging and high predisposition to cancer. Cells obtained from A-T patients display radiosensitivity, undergo premature senescence, and display faulty cell cycle checkpoint activation in response to irradiation (Beamish and Lavin, 1994; Chehab *et al.*, 2000; Falck *et al.*, 2002; Lavin and Shiloh, 1997; Lim *et al.*, 2000; Peng *et al.*, 1997; Xu *et al.*, 2002). After decades of research, a gene was found to be mutated in A-T patients and the gene product was responsible for the syndromes that A-T patients exhibited, so this gene was called Ataxia Telangiectasia Mutated (ATM) (Savitsky *et al.*, 1995).

Compared to other types of DNA lesions, DSBs are highly cytotoxic. In response to DSBs, cells execute cell-cycle arrest, in addition to activating DNA repair. When the lesions are too overwhelming to repair, apoptosis will be activated (van Gent *et al.*, 2001). A complicated network in the cell mediates all these activities, and ATM plays the most crucial role in it. A trimeric protein complex, Mre11-Rad50-Nbs1 (MRN) is shown to act as a DSBs sensor and recruit ATM to the breakage sites, although the exact mechanism of how the DNA damage signal is conveyed to ATM has yet to be elucidated (Lee and Paull, 2004; Lee and Paull, 2005). DSB is shown to induce intermolecular auto-phosphorylation of ATM kinase at serine 1981, which dissociates the inactive dimer of ATM and initiates kinase activity of ATM (Bakkenist and Kastan, 2003). DSB-activated ATM kinase phosphorylates numerous substrates including p53, c-Abl, BRAC1 to regulate cellular responses. All ATM substrates contains a general consensus motif – serine or threonine that is followed by a glutamine (SQ/TQ motif) (Kim *et al.*, 1999b). Until now, there have been more than a dozen substrates of ATM found *in vivo*, and this list keeps increasing with further investigation of ATM. Among them, p53 is the best studied substrate of ATM, as well as c-Abl (Baskaran *et al.*, 1997; Shangary *et al.*, 2000).

Following IR-induced activation, ATM directly phosphorylates p53 on serine 15 leading to stabilization. ATM activates protein kinase, Chk2 by phosphorylation on threonine 68, which in turn phosphorylates p53 on serine 20 (Banin *et al.*, 1998; Matsuoka *et al.*, 2000). These dual phosphorylations prevent p53 from degradation by inhibiting ubiquitination of p53 executed by ubiquitin ligase MDM2 (Shieh *et al.*, 1997; Unger *et al.*, 1999). This stabilization is crucial to p53's function as a tumor suppressor and transcription factor. Consequently, lack of ATM-mediated p53 phosphorylation is responsible for the blunted up-regulation of p21^{WAF-1/CIP-1} and defective G₁/S cell arrest observed in irradiated A-T cells (Di Leonardo *et al.*, 1994; el-Deiry *et*

al., 1993). In addition, ATM regulates p53 levels by phosphorylating MDM2, weakening MDM2-p53 interaction and promoting p53 induction (Maya *et al.*, 2001). Furthermore, ATM-dependent phosphorylation of p53 on residues serine 46 and serine 9 are documented to be important for p53-mediated apoptotic response to radiation treatment (Saito *et al.*, 2002).

In summary, ATM regulates an intricate network in response to DNA damage through phosphorylation and activation of multiple substrates. Further understanding of ATM and its substrates is anticipated to broaden our knowledge of cancer initiated by unrepaired DNA damage and provide novel targets for pharmaceutical therapy.

2.1.2 p53 acetylation

Acetylation is another post-translational modification that controls p53 activity in response to genotoxic stress (Sakaguchi *et al.*, 1998). Gu *et al.* reported that p53 is acetylated at multiple lysine residues (K373/K382) on its carboxyl-terminal regulatory domain, and that this acetylation stimulates the sequence-specific DNA-binding activity of p53 (Gu and Roeder, 1997). Subsequent studies showed that, *in vivo*, p53 can be acetylated on both on N-terminal and C-terminal domains in response to a variety of cellular stress signals including IR, UV, hydroxyurea and hypoxia (Gottifredi *et al.*, 2001; Gu and Roeder, 1997; Ito *et al.*, 2001; Liu *et al.*, 1999; Sakaguchi *et al.*, 1998).

2.1.3 Acetyltransferase

The principal enzymes implicated in p53 acetylation are the transcriptional co-activator p300 and its close family member CREB Binding Protein (CBP). p300 and CBP are distinct, but related, proteins that participate in a wide variety of cellular process, including proliferation, differentiation and apoptosis (Avantaggiati *et al.*, 1997; Puri *et al.*, 1997; Yuan *et al.*, 1996). Owing to their intrinsic acetyl-transferase activity, p300 and CBP facilitate chromatin remodeling through histone acetylation (Bannister and Kouzarides, 1996). Thus, this post-translational modification has emerged as a key mechanism in regulating gene expression (Ogryzko *et al.*, 1996). Mice deficient in either p300, CBP or both display embryonic lethality while heterozygotes exhibit defects in growth and development (Yao *et al.*, 1998), indicating a role for p300/CBP in embryonic development. Cells deficient in p300 display radiosensitivity and impaired apoptotic response to IR exposure implying a critical function for this molecule in DNA damage response (Yuan *et al.*, 1999). In humans, deregulation of p300 and CBP activities are reported to cause some specific types of leukemia (Gayther *et al.*, 2000). Additionally, patients with Rubinstein-Tayabi syndrome exhibiting developmental abnormality and skeletal deformity are heterozygous for mutation in the CBP allele (Petrij *et al.*, 1995). CBP heterozygous mice also show skeletal abnormalities reminiscent of Rubinstein-Tayabi syndrome (Tanaka *et al.*, 1997).

2.1.4 Summary

Both p300 and ATM-deficient cells are sensitive to radioactivity (Lavin and Khanna, 1999; Pacini *et al.*, 1999). This prompted us to investigate a potential role for ATM in

controlling p300 function in response to IR. As outlined in this study, we show that Histone Acetyl-Transferase (HAT) activity of p300 is elevated in response to IR in an ATM-dependent manner. In agreement with this, we observed impaired p53 acetylation in ATM-deficient cells after IR. Using both *in vivo* and *in vitro* approaches we show that p53 phosphorylation kinetically precedes acetylation and that phosphorylation enhances p53 as a substrate for p300 acetyltransferase. Importantly, we demonstrate that ING2 participates in the acetylation of p53 and in addition required for activation of p300 HAT activity. Together, the results demonstrate ATM as an upstream regulator of p300 HAT activity mediating through ING2 in the IR-induced signaling pathway and that p53 is modified by phosphorylation/acetylation in a concerted manner.

2.2 MATERIALS AND METHODS

2.2.1 Cell Culture

Normal (GM00730) and A-T (GM02530) human fibroblasts were obtained from Coriell Institute for Medical Research (Camden, NJ) and Cultured in DMEM supplemented with 10% fetal bovine serum (FBS), 5% essential amino acids, 2% non-essential amino acids, vitamins, 100 units/ml pen/strep and 5 mM L-gultamine. Normal (GM0536B) and A-T (GMO1525E) lymphoblastoid cell lines were obtained from NIGMS Human Genetic Mutant Cell Repository (Camden, NJ) and cultured in RPMI-1640 supplemented with 15% heat inactivated FBS, 100 units/ ml pen/strep and 5mM L-Glutamine (Ziv *et al.*, 1997). SV-40 transformed A-T fibroblast cell line AT22IJ-T stably expressing full-length recombinant ATM (designated as YZ-5) or

stably transfected with empty vector (designated as EBS-7) were cultured as described by Ziv *et al* (Ziv *et al.*, 1997). The p53 inducible Tet-off cell line LNZ-308 was cultured in DMEM supplemented with 10% FBS, 100 unites/ml pen/strep and 5 µg/ml tetracycline as described (Gossen and Bujard, 1992). All cell lines were maintained at 37°C in a humidified 5% CO₂ incubator.

2.2.2 Irradiation

Exposure of cells to different doses of γ -radiation was performed at room temperature using a Gammacell 1000 Irradiator (Atomic Energy of Canada Ltd) equipped with a ¹³⁷Cs source (dose rate = 318 rad/min). After irradiation the media was changed and cells returned to the incubator, and harvested at indicated time points.

2.2.3 Reagents and Antibodies

Caffeine and wortmannin were purchased from Sigma Chemical Company (St Louis, MO). Where indicated, cells were pretreated with 5 mM caffeine or 10 µM wortmannin in serum-free media for 1 hour at 37°C before irradiation. Lys-CoA was synthesized according to the published method of Lau *et al* (Lau *et al.*, 2000), purified by HPLC (c-18 colum), and analyzed by mass spectroscopy. The inhibitory effects of the purified Lys-CoA were confirmed in *in vitro* acetylation reactions using immunoprecipitated p300 and purified histones as substrates.

The anti-acetylation lysine antibody PAN-193 (ab-193-100) was purchased from Upstate Biotechnology (Lake Placid, NY). Polyconal anti-p300 (sc-584), anti- β -tubulin (sc-935) and

monoclonal anti-p53 (DO-1, sc-126) antibodies were obtained from Santa Cruz Biotechnology. Phospho-specific anti-p53-Ser15 (9284 S) was purchased from Cell Signaling (Beverly, MA). ING2 antibody (rat, monoclonal) was a generous gift from Dr. Or Gozani at Stanford University.

2.2.4 Reversible cell permeabilization

Cells were treated with Lys-CoA as described by Bandhopadhyay et al. (Bandyopadhyay *et al.*, 2002). Briefly HEK-293 cells (5×10^6) were trypsinized and resuspended in 1 ml of ice-cold buffer (ICB) containing 10 mM HEPES, pH 7.0, 0.14 M KCl, 0.01M NaCl and 2.4 mM $MgCl_2$. 50 μ l of ICB solution containing 0.5% trypan blue with or without Lys-CoA was added to 500 μ l of cell suspension containing 50 μ l transport reagent (1.2 mg/ml sphingosylphosphorycholine) and subsequently incubated at 37°C for 30 minutes. Following this 100 μ l of stop reagent (20% fatty acid-free BSA in ICB) was added and cells seeded in 60 mm dishes in 5 ml of complete growth media and placed in a 37°C incubator. Following 12 hr incubation, cells were re-fed with fresh media and cultured for 24 to 48 hr prior to IR exposure.

2.2.5 Immunoblotting

Cells were harvested by scraping, washed with ice-cold PBS, and lysed in cold 1X lysis buffer containing 10 mM Tris HCl pH 8.0, 240 mM NaCl, 5 mM EDTA, 1 mM DTT, 0.1 mM PMSF, 1% Triton X-100, 1 mM sodium vanadate, and 1 μ g/ml of leupeptin, pepstatin, and aprotinin by incubation on ice for 20 min. Lysates were cleared by centrifugation and protein concentration was determined using Bradford dye reagent from BioRad. For immunoblotting, proteins were resolved by SDS-PAGE on 4-12% gradient gels, electro-transferred to Immobilon-

P (Millipore, Billerica, MA) membranes and probed with indicated primary antibody and subsequently with HRP-conjugated secondary antibodies. The membrane was developed using chemiluminescence reagent Luminol. Where indicated, the membrane was stripped by incubation at 40°C for 30 min in 65 mM Tris-HCl pH 6.7, 100 mM β -mercaptoethanol (BME) and 2% SDS and then probed with indicated antibody.

2.2.6 Immunoprecipitation

Immunoprecipitation was performed as described (Shangary *et al.*, 2000). Briefly, 1×10^6 cells were lysed in 500 μ l of 1X lysis buffer (20 mM Tris-HCl, pH7.5 / 150 mM NaCl / 5 mM EDTA / 0.5% NP40 / 1 mM NaF / 1 mM DTT / 1 mM Na-Vanadate) and clarified by centrifugation. Lysates were adjusted for equal protein content and 5 μ l of antibody (anti-p300 / anti-ING2/ anti-ATM) was added, and incubated overnight at 4°C on a rocking platform. 25 μ l of 50/50 (v/v) slurry of protein A-Sepharose beads (American Pharmacia Biotech) in PBS was added and incubation continued for another 2 hours. Immune-complexes were collected by quick spin, washed three times in 1x lysis buffer containing 500 mM NaCl, once with 1X lysis buffer, and subsequently used in HAT assays or analyzed by SDS-PAGE and immunoblotting.

2.2.7 Histone Acetyltransferase (HAT) Assay

HAT assays were performed as described by Zeng *et al.* (Zeng *et al.*, 2000). p300 immune-complexes were washed once in HAT buffer (50 mM Tris-HCl, pH 8.0 / 10% glycerol (v/v) / 1 mM DTT / 0.1 mM EDTA / 10mM sodium butyrate / protease inhibitors) and

resuspended in 20 μ l of HAT buffer. 5 μ g of calf thymus histones (Boehringer Mannheim), 1 μ M acetyl CoA and 50 Ci of 14 C-Acetyl CoA (ICN, 55mCi/mM) were added, and the reaction mixture was incubated for 45 min at room temperature. The reaction was terminated by addition of 25 μ l SDS-sample loading buffer and immersion in a boiling water bath. The proteins were resolved by 4-12% SDS-PAGE, electrotransferred onto Immobilon-P membrane. Radiolabeled substrates were visualized by autoradiography. Enzyme abundance in each reaction was confirmed by immunoblotting with anti-p300 antibody

2.2.8 *In vitro* ATM Kinase Assay

ATM kinase assay were carried out as described (Shangary *et al.*, 2000). Mock (DMSO) and IR-treated cells or control cells were harvested 1 hour post-irradiation. Lysates were prepared as described and normalized for equal protein content. Lysates were immunoprecipitated by incubating with 5 μ l of anti-ATM antibody for 2 hours on a roto-mixer at 4°C. 25 μ l of 50/50 (v/v) slurry of protein A-sepharose beads in PBS were added and incubation continued for 2 hours at 4°C. The beads were collected by quick spin, washed twice with lysis buffer and once with 100 mM NaCl supplemented with protease inhibitors. The beads were resuspended in 25 μ l of kinase buffer (25 mM HEPES, pH 7.5, 50 mM KCl, 0.5 mM EDTA, 5 mM DTT, and 0.5 mM phenylmethylsulfonyl fluoride). The beads were incubated with 1 μ g of purified recombinant GST-p53, 5 mM cold ATP and 30mCi of [γ - 32 P] ATP (5000 mCi/mM ICN) and incubated at 30°C for 30minutes. The reaction was terminated by addition of 25 μ l of SDS-sample loading buffer and boiling for 10 minutes. The reaction products were resolved on 10% SDS-PAGE, electrotransferred on Immobilon-P (Milipore) membranes and analyzed by autoradiography.

2.2.9 RNA interference

Overlapping synthetic oligonucleotides corresponding to sequences specific for the human ING2 (5'– AGAGAGCACTAATTAATAG -3') transcripts were hybridized and cloned into pSIREN-RETRO-Q (Clontech, La Jolla, CA). The recombinant pSiren plasmid was co-transfected with pCL-ampho plasmid encoding the packaging viral DNA into the packaging cell line, 293T (Clontech) using Lipofectamine 2000 (Invitrogen, Carlsbad, CA). The supernatant containing the viral DNA was collected, filtered and used to infect HCT-116 cells with polybrene-supplemented medium. Cells were selected by incubation with puromycin (1 µg/ml) for 4 days and downregulation of target gene expression was confirmed by immunoblotting.

2.2.10 Microscopy

Cells were grown on pre-sterilized glass cover slips and either mock- treated or exposed to IR (5 Gy). Cells were then washed 3x with Hank's Balanced Salt Solution (HBSS) containing 10 mM HEPES, 2 mM CaCl₂, and 4 mg/ml BSA. Cells were fixed in 4% paraformaldehyde in HBSS for 5 min and then permeabilized in 100% methanol for 5 min. Cells were then stained with ING2 antibody (rabbit) for 1 hr at 37°C. The cells were subsequently stained with Alexa Fluor 555 goat anti-rabbit IgG-conjugated secondary antibody (Invitrogen, Carlsbad, CA). DNA was counterstained with DAPI. Photomicrographs were recorded using a Nikon fluorescence microscope (TE S2000) equipped with CCD camera.

2.3 RESULTS

2.3.1 IR induces p300 histone acetyltransferase activity.

Genotoxic agents such as ionizing and ultraviolet radiation induce acetylation of a number of proteins including p53, p73 and E2F-1, mediated by HAT activity of p300/CBP (Gottifredi *et al.*, 2001; Gu and Roeder, 1997; Ito *et al.*, 2001; Liu *et al.*, 1999; Sakaguchi *et al.*, 1998). To identify the mechanism leading to increased acetylation of proteins after DNA damage, we monitored alterations in p300 HAT activity. Logarithmically grown HEK-293 cells were exposed to 5 Gy (500 rad) of IR and p300 Histone Acetyltransferase (HAT) activity was determined by immunoprecipitation followed by incubation of IP-complex with histones and ^{14}C acetyl CoA in an *in vitro* HAT assay. Stringent conditions were used for immunoprecipitation so that no other HAT proteins such as PCAF could be co-precipitated with p300. As shown in Figure 1A, p300 immunoprecipitated from IR-exposed cells displayed increased HAT activity as demonstrated by increased incorporation of ^{14}C onto histones. Untreated cells showed only a basal level of HAT activity. The presence of comparable levels of p300 protein in control and IR-treated cells (Figure 2A *bottom panel*) showed that the acetyl transferase activity is in fact stimulated during DNA damage. Quantitation of ^{14}C incorporation onto histones revealed ~3.5, 5, 6.1 and 5.8 fold increase in p300 HAT activity at 1, 2, 4 and 8 h post-IR respectively. Activation was dose-dependent: increasing doses of IR exposure led to higher HAT activities (Figure 2B). In contrast to mock-treated, IR-exposed cells showed 3.5, 3.6, 3.7 and 6.1 fold increases in p300 HAT activities in response to 5, 10, 15 and 20 Gy of IR, respectively. Together, these results showed that p300 HAT activation proceeds in both time- and dose-dependent manner.

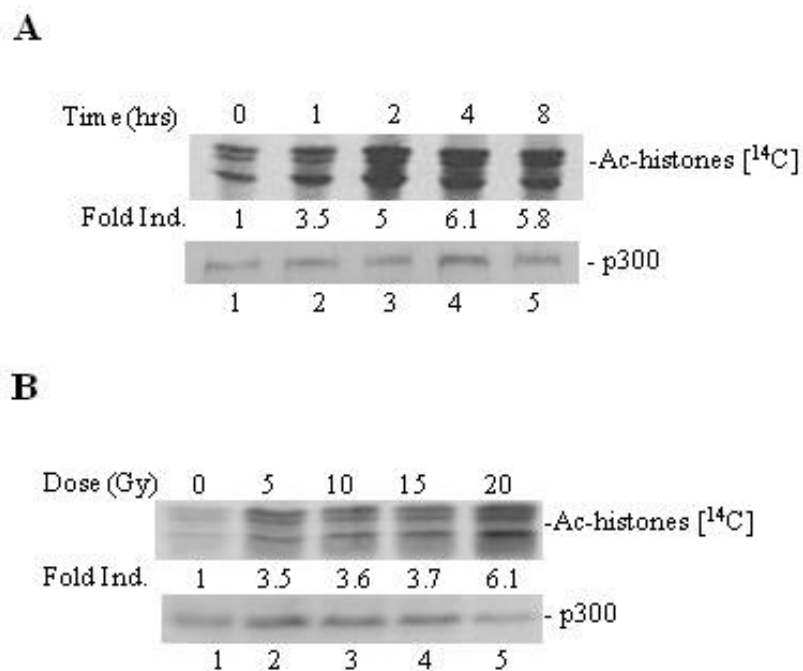


Figure 2: Time and dose-dependent activation of p300 HAT activity by IR.

(A) HEK-293 cells were irradiated with 5 Gy of IR, and harvested 0, 1, 2, 4, and 8 h later. Lysates were formed, adjusted for equal protein content. Subsequently, p300 was immunoprecipitated from these lysates and HAT activity was measured by incubating immunoprecipitated-p300 with histones in presence of [¹⁴C] acetyl-CoA. The reaction products were resolved by 12% SDS-PAGE, transferred onto Immobilon-P. The radio-labeled bands were detected by autoradiography. The top portion of the membrane was probed with anti-p300 antibody to assure equivalent acetyltransferase abundance. (B) HEK-293 cells were exposed to 5, 10, 15 and 20 Gy of IR and lysates were formed 1 h after irradiation. p300 was immunoprecipitated from these lysates, and HAT activity was assessed as described in panel A. p300 abundance was determined by immunoblotting.

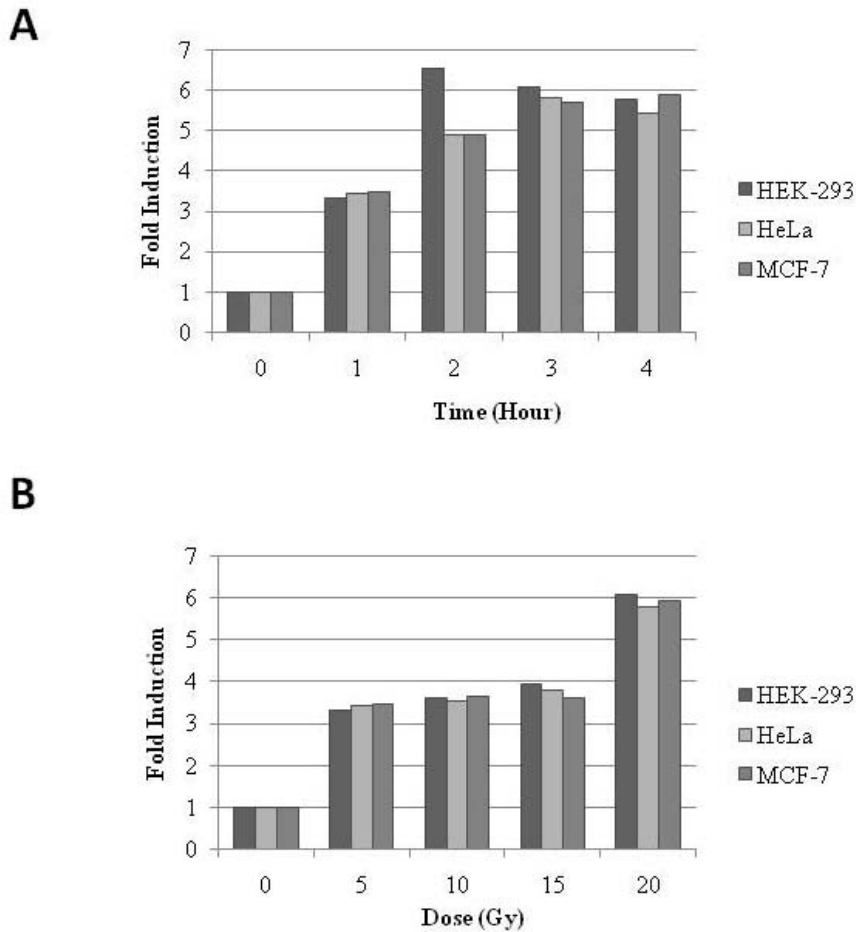


Figure 3: Time and dose-dependent p300 HAT activation in HEK-293, HeLa and MCF-7 cells following IR exposure.

(A) HEK-293, HeLa and MCF-7 cells were exposed to 5 Gy of IR and HAT activity was assessed as described in Figure 2. (B) HEK-293, HeLa and MCF-7 cells were exposed to 5, 10, 15, 20 Gy of IR and HAT activity was measured 1 hr after. Fold activation was determined by densitometric scanning of the labeled histone bands using a phosphor-imager analysis.

2.3.2 IR-induced p300 HAT activation is not cell-line specific.

To determine whether p300 activation induced by IR proceeds in a non cell-type specific manner, we conducted parallel HAT assays in HeLa and MCF-7 cells. Similar to the results attained in HEK-293 cells, activation in response to IR exposure occurred in both cells. Importantly, both the cells showed time and dose-dependent activation of p300 HAT activity in response to IR exposure (Figure 3).

2.3.3 ATM is required for IR-induced p300 HAT activity upregulation.

ATM and ATR kinases critically modulate cellular responses to DNA damage through phosphorylation and activation of a number of downstream molecules. To evaluate their involvement in p300 HAT activation, we tested the effect of caffeine, an ATM/ATR kinase inhibitor on IR-induced p300 HAT activation. HEK-293 cells were exposed to IR in the presence of caffeine and p300 HAT activation was assessed by HAT assay. As shown in Figure 4, caffeine treatment blocked p300 HAT activation. Whereas cells exposed to IR showed ~3.5 fold increase in p300 HAT activity, caffeine-treated cells showed ~1.5 fold increase in p300 HAT activity (Figure 4, *compare lane 2 to 4*). We next examined if ATM function is specifically required for p300 HAT activation by IR. We compared HAT activation in normal (GM 00730) and A-T fibroblasts (GM 02530, ATM-deficient). Compared to normal fibroblasts cells which displayed 6.5 fold p300 HAT activation, A-T fibroblasts showed no increase in HAT activation by IR (Figure 5A, *top panel*). Anti-p300 immunoblotting of the lysates obtained from these cells showed p300 levels comparable to normal cells (*bottom panel*). In a parallel experiment, HAT activity in normal (GM0536B) and A-T lymphoblastoid cells (GM01525E) was also examined.

Similar to the results observed in fibroblast cells, p300 HAT activity displayed a clear increase after IR in normal lymphoblasts while no p300 HAT activation was seen in A-T deficient lymphoblastoid cells (Figure 5B). To confirm the ATM requirement, we examined p300 HAT activation in SV-40 transformed AT-fibroblasts expressing recombinant human ATM (designated YZ-5) and cell line stably transfected with empty vector (designated EBS-7). Indicating a requirement for ATM function, p300 obtained HAT activity in EBS-7 showed no HAT activation whereas ATM reconstituted YZ-5 cells exhibited ~3.9 fold increase in HAT activity (Figure 5C). Taken together, these results indicate a requirement for ATM function in p300 HAT activation induced by IR.

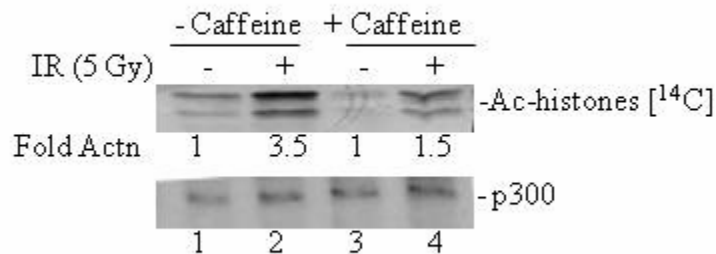


Figure 4: p300 HAT activation in the presence or absence of caffeine post-IR
 HEK-293 cells were either untreated or pretreated with 5 mM caffeine and exposed to 5 Gy of irradiation. One hour after IR, the cells were harvested and HAT activity and p300 abundance were measured.

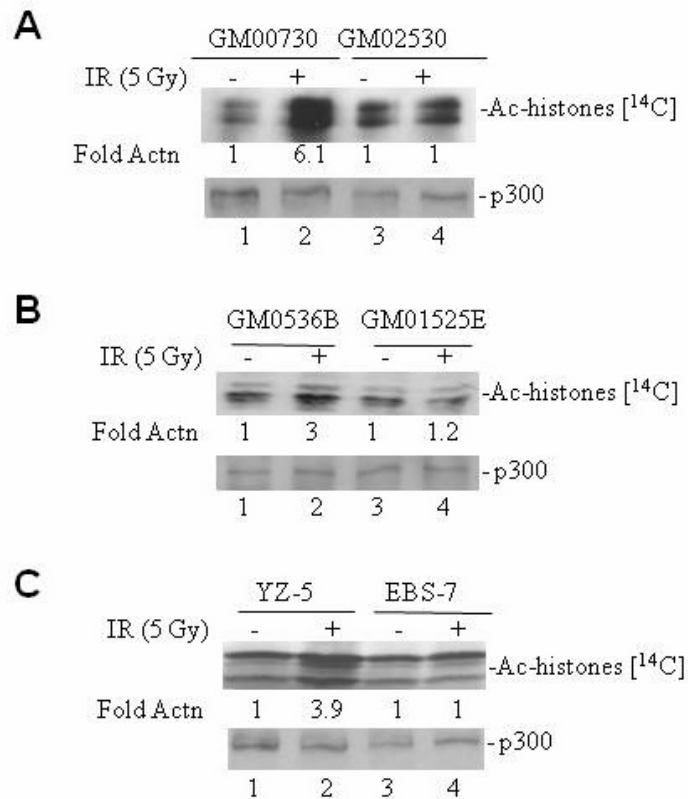


Figure 5: IR-induced p300 HAT activation requires ATM.

(A) Normal (GM00730) and ATM deficient fibroblasts (GM02530) were either exposed to 5 Gy of IR or were unexposed and p300 HAT activity and p300 abundance measured 1 hr after IR. (B) Normal (GM0536B) and ATM deficient lymphoblastoid (GM01525E) cells were analyzed for irradiation-induced (5 Gy, 1 hr after IR) activation of p300 HAT activity. (C) p300 HAT activity was measured in the SV-40 transformed isogenic fibroblast lines ATM-proficient YZ-5 and ATM-deficient EBS-7 1 hr after exposure to 5 Gy of irradiation.

2.3.4 Acetylation of p53 after IR is an ATM-dependent process.

To demonstrate the relevance of IR-induced and ATM-dependent upregulation of p300 HAT activity, we examined the acetylation of one of its substrates, p53 (Ito *et al.*, 2001; Liu *et al.*, 1999; Sakaguchi *et al.*, 1998). Since p53 can be acetylated on multiple residues, we first examined the total acetylation of p53. Extracts formed from HEK-293 cells at various times after IR exposure were used to immunoprecipitate p53 using anti-p53 antibody and probed with anti-acetyl lysine antibody (PAN-193). We found that irradiation resulted in acetylation of p53 at 2 and 4 hr post-treatment (Figure 6, *top panel*). Consistent with activation of ATM after irradiation, we also observed the phosphorylation of p53 on serine 15 as well (Figure 6, *bottom panel*). Thus, normal response to IR exposure includes coordinated phosphorylation and acetylation of p53.

When we tested the effect of caffeine and wortmannin, we detected that IR-induced p53 acetylation was completely abrogated in cells pretreated with caffeine (Figure 7A, *top panel*). Of note, caffeine pretreatment had a quantitative effect on accumulation of Ser15-phosphorylation but did not completely block this irradiation-induced event (Figure 7A, *bottom panel*). Likewise, normal fibroblasts pretreated with wortmannin inhibited IR-induced acetylation (Figure 7B, *top panel*) and Ser15 phosphorylation (Figure 7B, *bottom panel*) of p53. Comparing p53 acetylation and Ser15 phosphorylation in normal (Figure 7C, *lane 1-4*) and A-T (Figure 7C, *lane 5-8*) fibroblast lines revealed a significant reduction in both IR-induced acetylation and phosphorylation of p53 in A-T cells. Taken together, the inability of ATM-deficient cells to upregulate p300 HAT activity and acetylate p53 in response to ionizing radiation strongly suggests that, in addition to phosphorylating p53, ATM directs p53 acetylation after irradiation by upregulating p300 HAT activity. The inhibitory effect of caffeine and wortmannin on IR-

induced p53 phosphorylation and acetylation reinforced the requirement of ATM kinase in mediating these modifications.

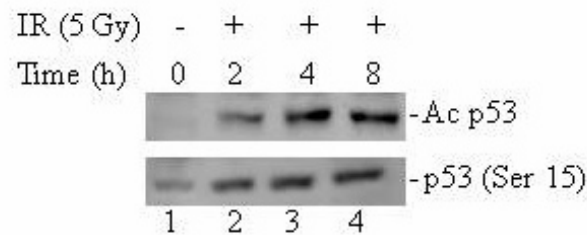


Figure 6: Time-course of p53 acetylation and phosphorylation in 293 cells after IR

HEK-293 cells were exposed to 5 Gy of irradiation and harvested 2, 4, 8 h later. The lysates from irradiated and unirradiated cells were subjected to immunoprecipitation with anti-p53 antibody. Subsequently, immunocomplexes were probed with anti-acetylated lysine (PAN 193) or anti-phosphorylated-p53 (Ser15) antibody. The membrane was stained with amido black after transfer to assure equal loading in all lanes.

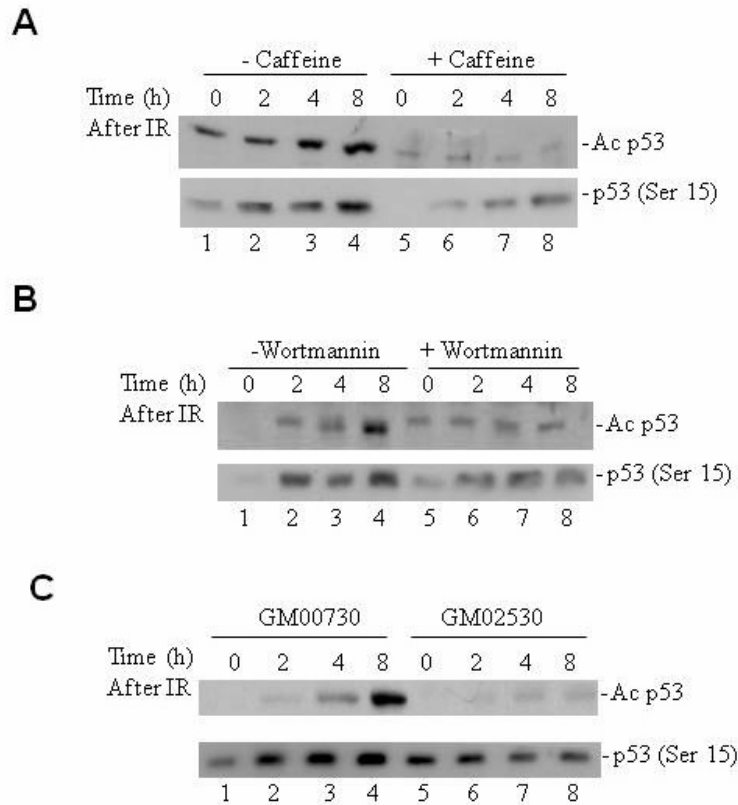


Figure 7: p53 acetylation after IR exposure is an ATM-dependent process.

(A) Normal (GM00730) fibroblasts were either untreated or pretreated with 5 mM of caffeine for 1 h and exposed to 5 Gy IR. The lysates were prepared and subjected to immunoprecipitation with anti-p53 antibody and subsequently stained for acetylated or phosphorylated (Ser15) p53 abundance. (B) Normal cells treated with wortmannin (and untreated cells were subjected to IR and the harvested cells were immunoprecipitated with anti-p53 antibody. Consequently, the immune-complexes were probed with anti-acetylated lysine or anti-phosphorylated-p53 (Ser15) antibody. (C) Normal (GM00730) and A-T (GM02530) fibroblasts were either unirradiated or exposed to 5 Gy of IR and harvested at indicated time points after irradiation, immunoprecipitated with anti-p53 antibody, and analyzed for acetylated p53 and Ser15 phosphorylated p53.

2.3.5 Phospho- p53 is a preferred target for p300.

IR exposure triggers phosphorylation of p53 on a number of residues and these events results in its stabilization and accumulation (Banin *et al.*, 1998; Canman *et al.*, 1998; Hirao *et al.*, 2000). Moreover, we have documented that irradiation leads to both phosphorylation and acetylation of p53 (Figure 6); thus, we investigated a potential role for p53 phosphorylation in directing p53 acetylation. We followed a time course of phosphorylation and acetylation of p53 in response to exposure to IR in HEK-293 cells (Figure 8A). We observed no detectable p53 acetylation 30 minutes after irradiation, modest acetylation 1 hour after irradiation and optimal acetylation 2, 4 and 8 hour after IR (Figure 8A, *top panel*). However, when we probed these extracts with anti-phospho-Ser15 p53 antibody (Figure 8A, *bottom panel*), we observed maximal Ser15 phosphorylation within 30 minutes after irradiation. This indicated that Ser15 phosphorylation precedes p53 acetylation in response to IR.

Next, we examined the co-operation of phosphorylation in the acetylation of p53 using both *in vivo* and *in vitro* approaches. We used recombinant p53 (GST-p53) as substrate and preformed *in vitro* kinase assay using immunoprecipitated ATM from irradiated cells. The GST-p53 beads were then subjected to *in vitro* acetylation using immunoprecipitated p300 from irradiated cells. Acetylation of GST-p53 was observed to be negligible in absence (Figure 8B, *top panel, lane 1 & 3*), but increased several folds in presence of phosphorylation (Figure 8B, *top panel, lane 2 & 4*).

We also used tetracycline-inducible (Tet-off) cell line (LNZ-308) to determine the kinetics of phosphorylation and acetylation of p53 in response to IR. When p53 was artificially induced in LNZ-308 by removing tetracycline (Figure 9A, *top panel*), there was no corresponding increase in either IR-induced phosphorylation or acetylation (Figure 9A, *middle &*

bottom panel). However, in response to γ -irradiation, LNZ-308 cells exhibited not only an induction of total p53 but also concomitant phosphorylation on serine 15 and associated p53 acetylation (Figure 9B). These results suggested an increase in p53 levels can't induce phosphorylation or acetylation without increased kinase and acetyltransferase activity. Taken together, these results clearly indicate that phosphorylation renders p53 a preferred target for p300-dependent acetylation in response to ionizing radiation.

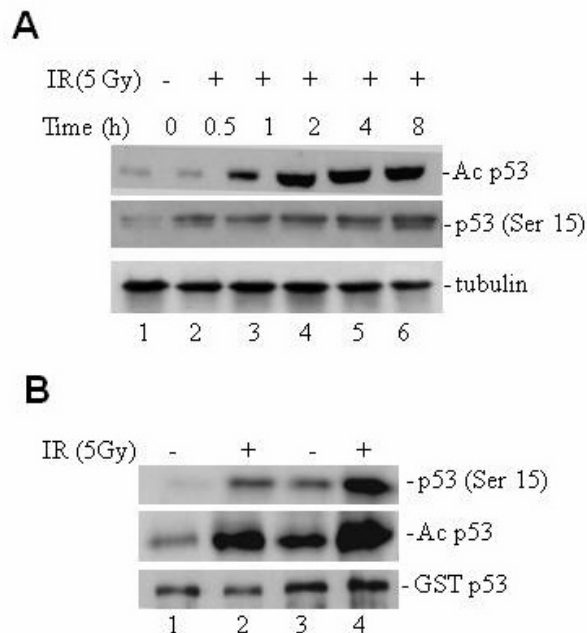


Figure 8: Phosphorylated p53 is a preferred substrate for acetylation.

(A) Time-course for HEK-293 cells after exposure to γ -radiation. HEK-293 cells were exposed to 5 Gy of IR and cell lysates prepared 0.5, 1, 2, 4 and 8 hours post-irradiation. These lysates from unirradiated cells were analyzed for acetylated p53 and phospho-Ser15-specific p53. (B) *In vitro* phosphorylation of GST-p53 followed by *in vitro* acetylation. Anti-ATM immunoprecipitates prepared from IR-treated or untreated cells were used to phosphorylate recombinant GST-p53 fusion protein *in vitro*. Subsequently, the product was re-purified and used as substrate in *in vitro* acetylation assays using immunoprecipitated p300. Total p53 was analyzed in the reactions to assure equivalent substrate in all reaction.

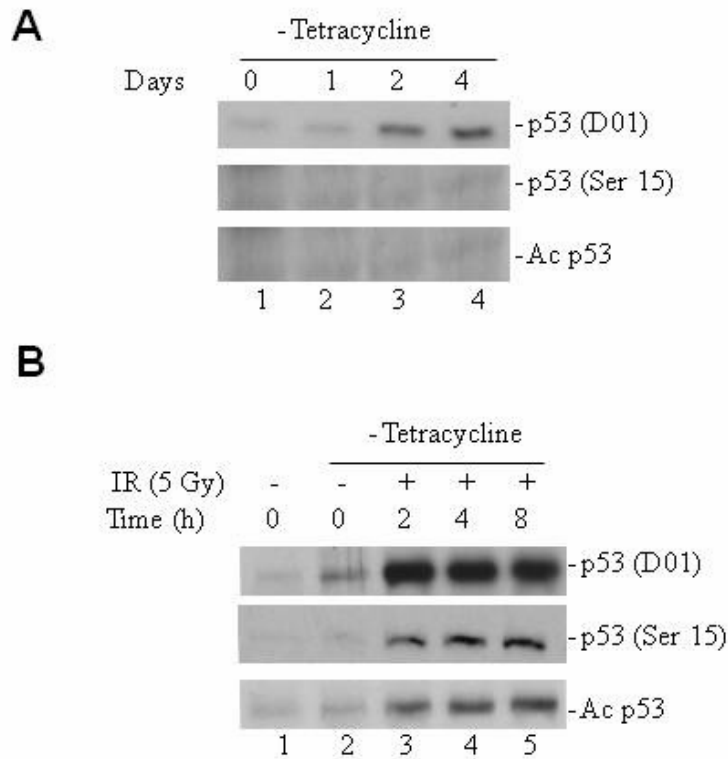


Figure 9: Increased p53 level is unable to upregulate p53 acetylation and phosphorylation without IR.

(A) p53 was synthetically induced in p53-deficient LNZ-308 glioma cells in absence of any exposure to γ -radiation by removing tetracycline from the cell medium. Harvested at 1, 2, and 4 days after drug removal, cell lysates were immunoprecipitated with total p53 (DO-1) antibody and examined for total, phosphorylated-p53 and acetylated-p53. (B) p53 was induced in LNZ-308 cells by subjecting them to 5 Gy of irradiation. Later the cells were harvested at 2, 4 or 8 hr post-IR, the lysates were immunoprecipitated with p53 (DO-1) antibody and analyzed for total, phosphorylated- and acetylated-p53.

2.3.6 IR-induced acetylation of p53 is regulated by two converse mechanisms.

To confirm the role of p300 HAT activity in regulating p53 acetylation, cells were treated with p300 HAT activity inhibitor, Lys-CoA, at different concentrations (0, 1, 10 mM) and p53 acetylation was assessed. At 1 mM concentration, Lys-CoA treatment decreased p53 acetylation by 50% and at 10 mM, a complete inhibition was observed (Figure 10A). Studies of Kim et al. (Kim *et al.*, 1999a) showed that ATM interacts with the histone deacetylase HDAC1 and the extent of this association is increased after exposure to ionizing radiation suggesting a possible contribution of ATM-mediated inhibition of HDAC1 activity to p53 acetylation. To evaluate the contribution of HDAC1 in driving p53 acetylation after IR exposure, we treated HEK-293 cells with increasing doses of HDAC 1 inhibitor, Trichostatin A (TSA), and examined IR-induced p53 acetylation. As show in Figure 10B (*top panel*), TSA treatment raised the basal level of p53 acetylation slightly in unirradiated cells. Further, at 4 and 8 hr post-IR, enhanced acetylation of p53 was observed (Figure 10B & 10C). Neither TSA nor Lys-CoA impacted p53 phosphorylation on S15 (Figure 10B, *bottom panel*). These results suggest that, p53 acetylation, in response to IR exposure, is simultaneously regulated by activating p300 HAT and conversely HDAC1 inhibition.

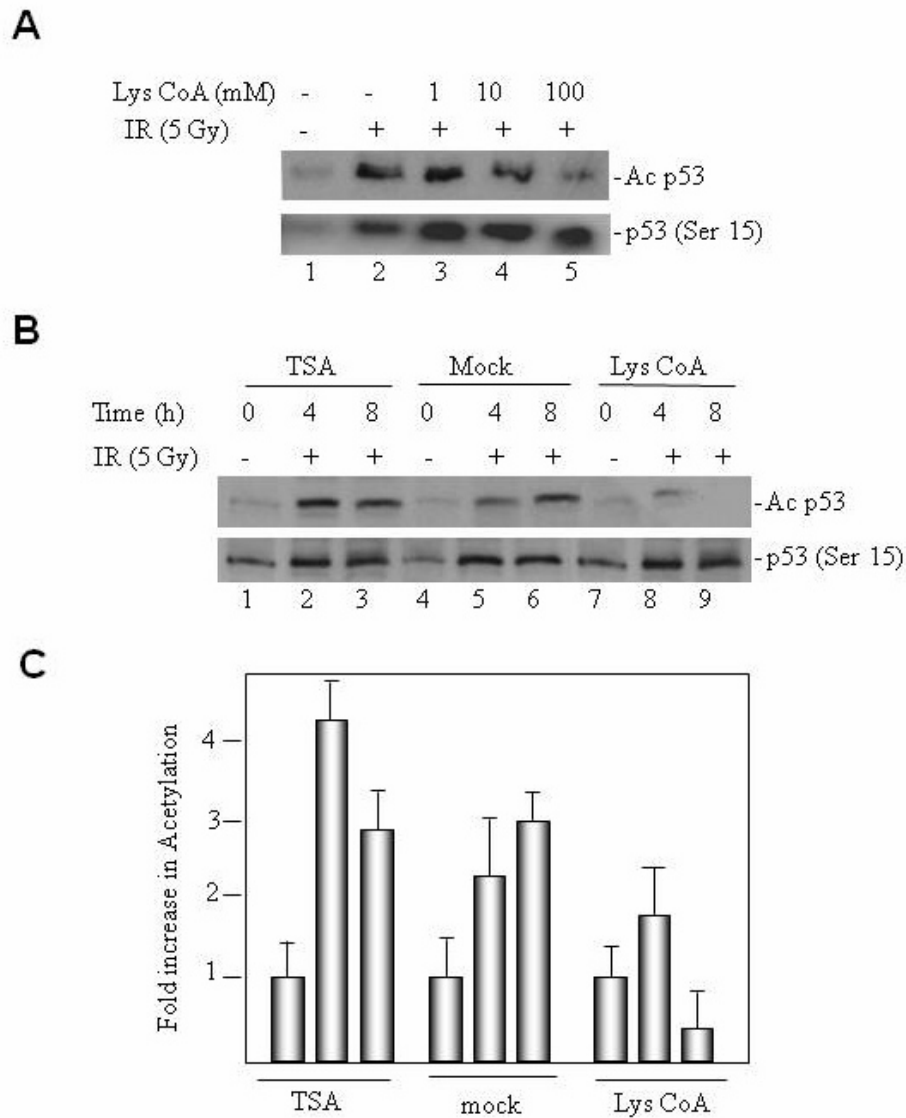


Figure 10: Effect of Lys-CoA and TSA on p53 phosphorylation and acetylation.

(A) Normal fibroblasts (GM 00730) pretreated with Lys-CoA at 1, 10 or 100 mM concentration were irradiated with 5 Gy of γ -radiation. The lysates were formed and were immunoprecipitated with p53 (DO-1) antibody and analyzed for acetylation or phosphorylation. (B) Normal fibroblasts (GM00730) pretreated either with Lys-CoA (100 mM) or Trichostatin A (1 μ M) or mock-treated were irradiated with 5 Gy of IR. Lysates

were formed and were immunoprecipitated with p53 (DO-1) antibody and analyzed for the presence of acetylated or phosphorylated p53. (C) Fold increase or decrease in acetylated level of p53 in Lys-CoA or TSA pretreated normal human fibroblasts subjected to 5 Gy of IR as compared to mock-treated cells was determined.

2.3.7 Relocalization of ING2 following γ -irradiation

ATM exerts its function as a signal transducer. Therefore, it is possible that ATM mediates p300 HAT activity through intermediate proteins. Harris *et al.* reported that ING2 promotes acetylation of p53 on lysine 320 after DNA damage caused by etoposide and neocarzinostatin (Nagashima *et al.*, 2001a). Thus, we examined the involvement of ING2 in p300 activation. ING2, a member of Inhibitor of Growth (ING) family, was found by homology search of another family member p33ING1b (Shimada *et al.*, 1998). ING family proteins are viewed as histone acetyltransferase and histone deacetylase co-factors, and participate in regulating transcription, cell cycle arrest, DNA repair and apoptosis (Campos *et al.*, 2004). Since ING2 was reported to enhance the acetylation of p53 after DNA damage, we hypothesized that ING2 increases the HAT activity of p300 after Ionizing Radiation (IR).

To that end, we examined intracellular ING2 protein levels after IR. Immunoblotting showed very little increase in ING2 protein level following irradiation (*data not shown*). Thus, subcellular distribution of ING2 in the cell was examined by immunofluorescence. Staining of cells with rat monoclonal anti-ING2 antibody revealed periplasmic nuclear staining in mock-treated control cells (Figure 11). However, within 4 hr after 5 Gy γ -radiation treatment we observed bright signaling both in the cytoplasm and nucleus. Merged images of DNA (DAPI

staining) and ING2 stained cells confirmed the relocalization of ING2 in response to IR exposure.

Taken together, the results demonstrated that although cellular levels of ING2 increased modestly, a clear translocation of ING2 from periplasm to cytoplasm and nucleus was observed following exposure to IR.

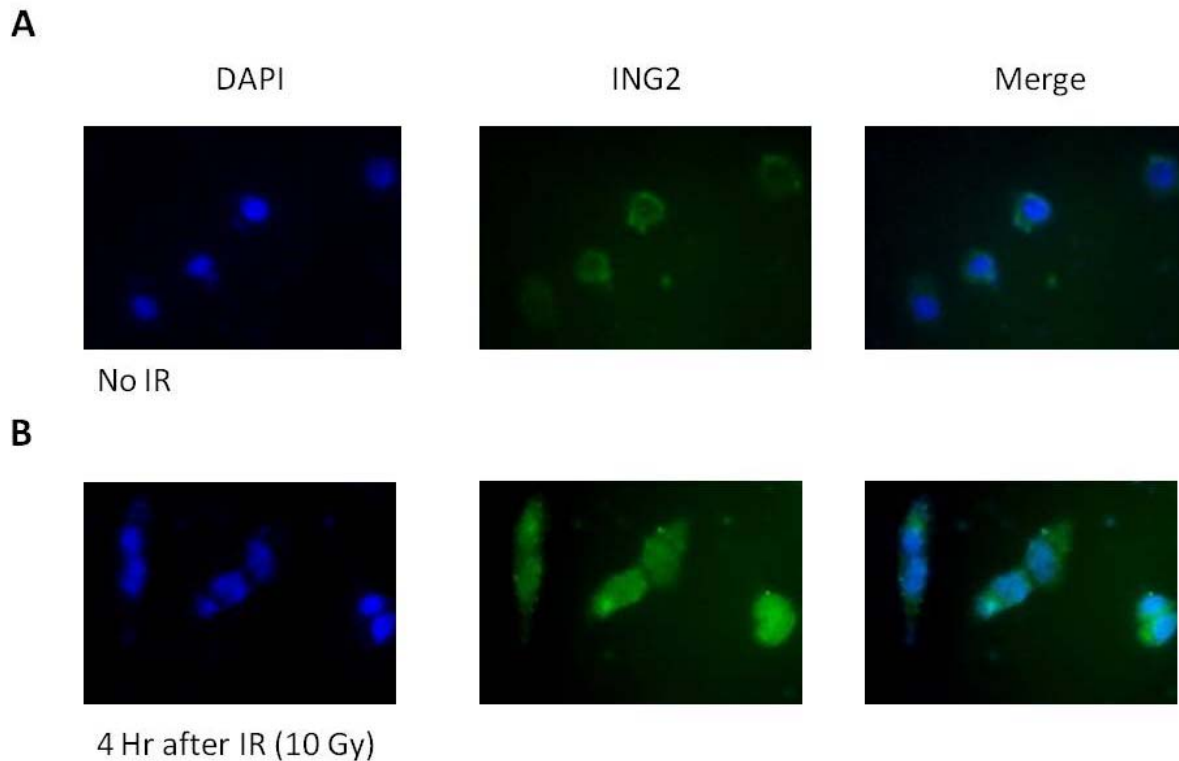


Figure 11: Relocalization of ING2 after IR

HeLa cells were grown on pre-sterilized glass coverslips and treated with DMSO (mock) or γ -irradiation 5 Gy. Four hours after treatment, cells were fixed, and stained with ING2 antibody (rabbit, red) for 1 hr at 37°C. Cells were subsequently stained with Alexa Fluor 555 conjugated goat anti-rabbit IgG secondary antibody. DNA was counterstained with DAPI (blue). Photomicrographs were recorded using a Nikon fluorescence microscope (TE S2000) equipped with CCD camera. Shown also is the merged image.

2.3.8 ING2 is required for the IR-induced p53 acetylation

To examine the involvement of ING2 in p300 HAT activation induced by IR, we suppressed ING2 expression in HCT116 cells using shRNA approaches as described in methods. As control, luciferase shRNA was used. Immunoblotting of the lysates prepared from control Luc- and ING2-knocked down cells confirmed suppression of ING2 protein expression in shING2 cells (Figure 12A). Subsequently, shING2 and control shLuc cells were exposed to 5 Gy of IR and p53 acetylation was assessed at 2, 4 and 8 hours post-treatment by immunoprecipitation. As anticipated, IR exposure induced a time-dependent increase in p53 acetylation in Luciferase knocked down cells. At each of the time point examined, ING2-knocked down cells showed low levels of p53 acetylation compared to shLuc cells (Figure 12B). Since p53 is the substrate of p300, p53 acetylation level can be used to measure p300 HAT activity. These results show decreased p53 acetylation following suppression of ING2 expression, suggesting a requirement for ING2 in p300 HAT activation in response to γ -radiation.

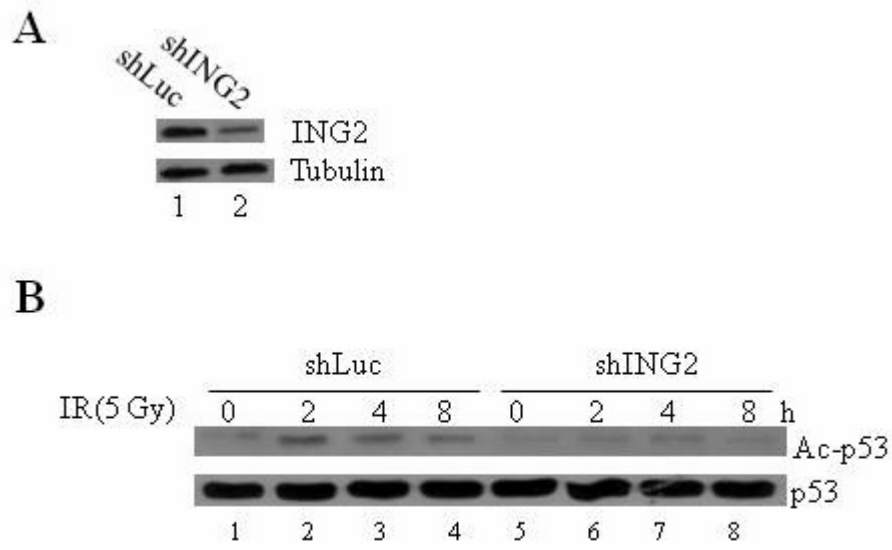


Figure 12: ING2 is indispensable for p53 acetylation induced by IR

(A) Lysates formed from shLuc and shING2 cells were subjected to immunoblotting with rat monoclonal anti-ING2 antibody. Anti- β -tubulin immunoblotting shows equal protein loading. (B) Control shLuc and ING2 knocked down shING2 cells were exposed to 5 Gy IR. Cell lysates were prepared at 0, 2, 4 and 8 hours post-irradiation and subjected to immunoprecipitation with anti-p53 antibody and subsequently stained for acetylated or total p53 abundance.

2.3.9 p300 interacts with ING2 in an ATM-dependent manner.

ING2 activates p53 by enhancing its p300-dependent acetylation in replicative senescence (Pedeux *et al.*, 2005). In this process, ING2 functions as a scaffold protein increasing the association between p300 and p53. We documented that in response to irradiation, p300 HAT is activated and this upregulation requires ING2 function. These findings lead us to test the interaction between p300 and ING2 following irradiation by co-immunoprecipitation assay. Anti-p300 immunocomplex prepared from IR-treated cells showed the presence of ING2 (Figure 13A). The time course analysis showed optimal association at 2 hours after IR. Since ATM function was found to be indispensable for p300 HAT activation, we further investigated whether ATM is also required for the ING2 and p300 interaction. IR-induced association between ING2 and p300 was completely abrogated in HEK-293 cells pretreated with caffeine (Figure 13B), in agreement with the inhibitory effect of caffeine on p300 HAT activation. Comparing the association in normal and A-T fibroblast lines revealed a significant reduced interaction between ING2 and p300 in A-T cells compared to normal cells (Figure 13C). The inability of ATM-deficient cells to upregulate p300 HAT activity and to promote association between ING2 and p300 in response to ionizing radiation strongly suggests that ATM regulates p300 HAT activity through ING2. Perhaps, ING2 acts as an adaptor to promote interaction between ATM and p300 consequently stimulating p300 HAT activity.

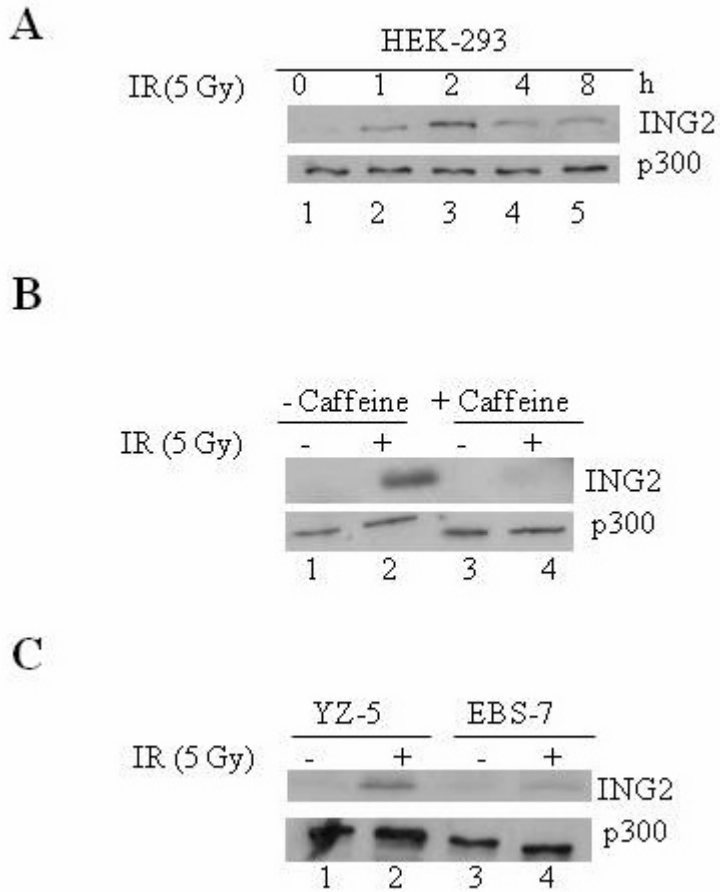


Figure 13: Association between ING2 and p300 post –IR requires ATM function.

(A) HEK-293 cells were exposed to 5 Gy of IR. Cell lysates were prepared at 0, 1, 2, 4 and 8 hours post-irradiation and subjected to immunoprecipitation with anti-p300 antibody and subsequently stained for ING2 association or p300 abundance. (B) HEK-293 cells were pretreated either with caffeine or were left untreated. The cells were irradiated with 5 Gy of IR and the lysates prepared 0 and 2 hours after IR from these and untreated cells were immunoprecipitated with p300 antibody and analyzed for the presence of ING2 or p300 abundance. (C) SV-40 transformed isogenic fibroblast lines ATM-proficient YZ-5 and ATM-deficient EBS-7 were either exposed to 5 Gy of IR. Lysates were harvested and prepared 0 and 2 hours post-irradiation from these cells, and

were immunoprecipitated with p300 antibody and analyzed for the presence of ING2 or p300 abundance.

2.4 DISCUSSION

Acetylation modification has emerged as an important mechanism for activation of apoptosis in response to genotoxin-induced DNA damage. However, the signaling events leading to this modification remains unclear. In this part, we document that exposure of cells to IR upregulates p300 HAT activity and that IR-activated p300 acetylates p53 in an ATM-dependent manner. Consistent with this, treatment of cells with the ATM inhibitor, caffeine blocked p300 HAT activation and p53 acetylation induced by IR. Moreover, IR exposed A-T cells failed to activate p300 HAT activity and induce p53 acetylation. Restoration of ATM expression in A-T cells reinstated both these responses. Examination of requirement of ATM-mediated phosphorylation revealed that phospho-p53 is a preferred target for activated p300. Thus, these findings lead to conclude that ATM regulates p53 acetylation through a dual mechanism involving activation of p300 HAT and enhancing p53 as a target for HAT through phosphorylation.

2.4.1 p300 activation and phosphorylation

Given that ATM activates almost all of its downstream targets through phosphorylation, a plausible hypothesis would be that ATM stimulates p300 HAT through direct phosphorylation. However, immunoblotting of p300 purified from IR-exposed cells with an antibody that

recognizes S/T phosphorylated ATM substrates failed to bind (*data not shown*). Presumably, p300 is not a direct target of ATM kinase. A recent study has shown that phosphorylation of p300 by p38 MAP kinase activates its myogenic differentiation property (Bratton *et al.*, 2009). In addition, other kinases such as c-Abl and protein kinase C (PKC) has been implicated in DNA damage responses (Yoshida, 2007; Yoshida, 2008). Such findings raise the possibility these DSB responsive kinases may activate p300 through phosphorylation. The identification of p300 in BRCA1 complexes (Jeffy *et al.*, 2005) that is thought to act as a scaffold for mediating interaction with DNA repair molecules support the possibility that p300 may join DNA damage surveillance complex and that this association may facilitate its phosphorylation and activation of the repair components.

2.4.2 Role of ING2 in p300 HAT activation

Irrespective of phosphorylation, we have observed that ING2, implicated in p53 acetylation, is required for IR-induced p300 HAT activation. In support of this notion, we documented that suppression of ING2 expression attenuated p300 HAT activation in response to IR. Moreover ING2-knocked down cells displayed attenuated IR-induced p53 acetylation. These results allow us to conclude that, in addition to ATM, ING2 is yet another required component in the IR-induced activation of p300 HAT activity. Previous studies established that ING2 is documented to promote acetylation through its entry into complexes containing HDAC and HATs, thus acts as a scaffold to facilitate their interaction with acetylation targets at the DNA damage site (Doyon *et al.*, 2006; Shi *et al.*, 2006). Since co-immunoprecipitation assays showed enhanced interaction between p300 and ING2 following IR exposure, we propose that binding of ING2 to p300 may activate its HAT activity.

2.4.3 Functional Relevance of Plant Homeodomain (PHD) in ING2

The plant homeodomain (PHD) is a relatively small motif of ~60 amino acids that is found in >400 eukaryotic proteins, many of which are believed to be involved in the regulation of gene expression, including the KAP-1/TIF1 β , WCRF/WSTF, Mi-2 and CBP/p300 families (Aasland *et al.*, 1995). It has been suggested that this domain is involved in protein-protein interactions related to a possible role in chromatin-mediated regulation of gene expression (Jacobson and Pillus, 1999). The presence of PHD domains in both ING2 and p300 raise the possibility that p300 HAT activation could potentially be mediated by PHD-PHD interaction. In fact, the acetyl-transferase domain of p300 encompasses an analogous PHD domain (C/H2 as well as intervening sequence and the N-terminal part of C/H3). Thus, interaction at region may allow switching the more closed configuration of p300 to an open one, resulting in accessibility of acetylation of critical lysine residues which may otherwise be buried inside, consequently leading to increased auto-acetylation and hence increasing HAT activity. An open configuration may also provide increased accessibility to acetyl CoA and substrate binding (Figure 14). Consistent with this notion, we have observed that a correlation between increased auto-acetylation and increased HAT activity (*data not shown*). Of note, finer mapping of the regions required for HAT activity revealed that the plant homeodomain domain (PHD) of p300 which is originally mapped to the HAT domain of p300 (1195-1673) is shown to be dispensable for the *in vitro* acetylation activity of p300 (Bordoli et al 2001). Clearly, additional experimentations are required to fully elucidate the mechanism of p300 HAT activation induced by ING2 binding.

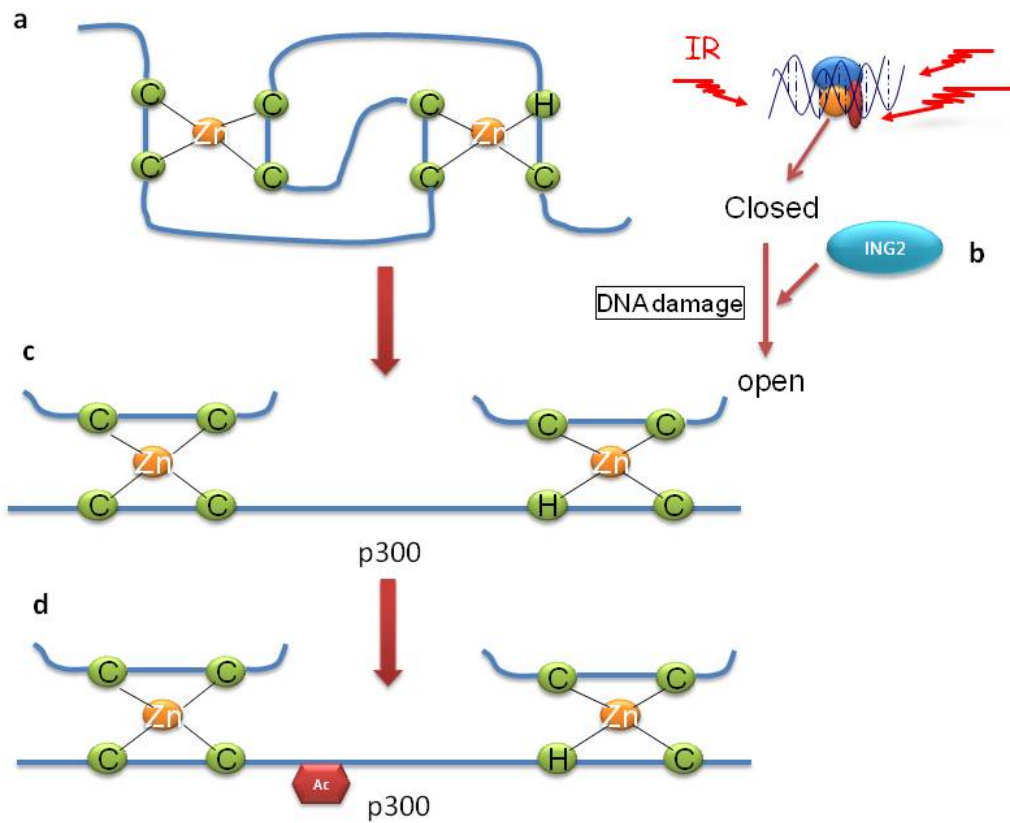


Figure 14: Proposed model for p300 HAT activation by ING2.

a) p300 maintains a closed inactive conformation in normal cells. **b)** Following IR, ING2 translocates into the nucleus and binds to p300. **c)** ING2 binding perturbs p300 thus unfolding and leading to an open conformation. **d)** This promotes auto-acetylation and activation of p300.

2.4.4 Functional role of p300 activation induced by IR in DNA repair

Loss of ATM is associated with radiosensitivity, a phenotype that is shared among cells deficient in DSB-repair (Shiloh, 2003). The radiosensitivity phenotype displayed by p300^{-/-} cells suggests that ATM-activated p300 may participate in repair of DSB breaks induced by IR. Thus, one possible function of IR-activated p300 may be to promote DNA repair through acetylation of DNA repair proteins. Importantly, p300 may also acetylate histones. Histone acetylation and consequential weakening of its interaction with DNA may allow sliding or falling off of histone to expose free naked DNA for repair complex entry facilitating repair. The recent finding that Ku70, a regulatory subunit of DNA-PK associates with p300 and is acetylated in an IR-dependent manner lends support to this possible function (Jeong *et al.*, 2007). An analogous scenario could also be visualized through its documented interaction with the breast cancer suppressor protein BRCA1 (Zhong *et al.*, 2002), which participates in homologous recombination (HR)-mediated DSB repair processes. In addition to directly contributing to DNA repair processes, p300 may also remodel chromatin through acetylation of its downstream target, such as p53 or p73 to facilitate DNA repair processes. The p53 has been proposed to function as a chromatin accessibility factor in the global genome repair (GGR) responses of the nucleotide excision repair (NER) pathway and p53 is shown to recruit p300 to sites of NER (Radic-Otrin *et al.*, 2002).

2.4.5 Functional Role of p300 activation induced by IR in apoptosis

In addition to activating repair process, DNA damage activates a cell death response. Activation of apoptosis occurs during irreparable DNA damage and in a cell-type specific manner. Critical components of the cell death machinery include p53, and its homolog p73. Interestingly, both, in addition to being phosphorylated, are also acetylated after IR and other DNA damaging agent treatment. Acetylation of p53 is associated with increased DNA binding and transcriptional activation of p53 since mutation of critical lysine (K120) residues necessary for acetylation sites blocks its ability to upregulate a host of pro-apoptotic genes including, PUMA, Bax and E2F1 (Sykes *et al.*, 2006; Tang *et al.*, 2006). Similarly, p73 acetylation is documented to corroborate with increased apoptotic activity (Costanzo *et al.*, 2002a). In sum, a host of pro-apoptotic genes including p21, MDM2, Cyclin-G, GADD45, IGFBP3 (A), IGFBP3 (B), Bax, PIGs, PERP, p53AIP1, NOXA, and the Killer/DR5 α have been show to mediate most of the effects of p53 and p73 (Pietsch *et al.*, 2008). Thus, DNA damage-activated p300 HAT may upregulate pro-apoptotic genes through acetylation and activation of p53 and p73's transcription function. The impaired cell death response observed in ATM-deficient cells raises the possibility that ATM-activated p300 may regulate the cell death response. In support of this observation, we have found that inhibition of p300 activation by Lys-CoA treatment blocked IR-induced apoptosis (*data not shown*). Moreover, A-T cells showed attenuated p53 acetylation after IR. It will be interesting to see if p73 is also acetylated in an ATM-dependent manner in response to γ -irradiation.

Together, results of our study show that p300 HAT activity is upregulated following genome damage and that ATM and ING2 are required for modulation of p300 HAT activity

towards p53. While phosphorylation of p53 by ATM facilitates its acetylation, ING2 is speculated to bind p300 thereby activating its HAT activity. Activated p300, in turn, promotes acetylation of key DNA repair and apoptotic mediator molecules through increased acetylation.

2.5 SUMMARY

Results of our study showed that p300 HAT activity is upregulated by γ -irradiation. The striking correlation between p300 activation and p53 acetylation, and the inhibition of p53 acetylation by Lys-CoA treatment clearly show that IR-activated p300 induces p53 acetylation. Further, the timing of p53 acetylation and phosphorylation and the preferential acetylation of phosphorylated p53 by p300 indicates that irradiation-induced post-translational modification of p53 is sequential in nature. Suppression of ING2 impairs the p300 HAT activation induced by ionizing radiation. Thus, ING2 is required for p300 HAT activation. The caffeine sensitive nature of the p300 HAT upregulation and the ATM-dependent association between ING2 and p300 indicates that ATM is a critical component in p300 HAT activation. In sum, IR-induced upregulation of p300 HAT is ATM- and ING2-dependent process.

**3.0 ING2 REGULATES MNNG-INDUCED APOPTOSIS THROUGH MMR/C-ABL-
DEPENDENT P73 ACETYLATION**

3.1 INTRODUCTION

3.1.1 Alkylating Agent: MNNG

DNA damage response mechanisms are crucial to limiting somatic mutations, maintaining genomic homeostasis, and limiting cancer development (Hartwell and Kastan, 1994; Loeb *et al.*, 2003). The monofunctional SN1 alkylating (methylating) agent, *N*-methyl-*N'*-nitro-*N*-nitrosoguanidine (MNNG) is an extremely mutagenic, carcinogenic agent that evokes multiple cellular responses including DNA repair, cell cycle arrest and apoptosis (Eadie *et al.*, 1984; Li, 2008; Loveless, 1969; Wyatt and Pittman, 2006). Although MNNG reacts with DNA to form several adducts, *O*-6-alkyl guanine, generated by alkylation of the DNA base, is the predominant cytotoxic and mutagenic lesion because of its mispairing properties (Eadie *et al.*, 1984; Loveless, 1969). Repair of the mutagenic O⁶MeG lesion by direct reversal is accomplished by the enzyme, methylguanine-DNA methyl-transferase (MGMT) (Foote *et al.*, 1980; Olsson and Lindahl, 1980). Lost or diminished MGMT activity increases MNNG-induced lesion load consequently raising cellular sensitivity to MNNG (Bobola *et al.*, 1995; Kalamegham *et al.*, 1988; Tominaga *et al.*, 1997).

3.1.2 Mismatch Repair System

The mismatch repair (MMR) system (Duckett *et al.*, 1996; Griffin *et al.*, 1994), an evolutionarily conserved DNA repair mechanism, chiefly responsible for resolving post-replicative mismatches in DNA (Modrich and Lahue, 1996), also recognizes and repairs O⁶MeG

lesions. It has been proposed that processing of O⁶MeG lesions by MMR during S phase gives rise to DNA double-strand breaks (DSBs) that finally provoke apoptosis (Meyers *et al.*, 2001). In addition to its capacity as a repair mechanism, numerous observations showed that MMR system is required for activation of signaling in response to persistent O⁶MeG lesions (Stojic *et al.*, 2004a).

The precise mechanism by which MNNG induces cell death is not known; however, numerous observations showed that MMR critically regulates signaling events that govern cell-cycle arrest and cell death induced by MNNG (Kim *et al.*, 2007; Stojic *et al.*, 2004a). MMR-deficient cells fail to upregulate p53 and p73 in response to DNA damage (Li, 2008). Although MNNG induces p53, its requirement in cell death is cell-type specific (Kim *et al.*, 2005; Li *et al.*, 2008). For example, lymphoblastoid cells expressing either a mutant form or ablated complement of p53 displayed heightened resistance to this alkylator. In p53 mutated gliomas, the same DNA lesion triggers the mitochondrial apoptotic pathway (Roos *et al.*, 2007). O⁶MeG-triggered apoptosis also requires Fas/CD95/Apo-1 receptor activation (Kaina *et al.*, 2007). A recent study showed that MMR-dependent intrinsic apoptosis is stimulated by hMLH1/c-Abl/p73 α /GADD45 α retrograde signaling (Li *et al.*, 2008). MNNG exposure also activates the PI-3 kinase, ATM (Adamson *et al.*, 2002) and ATM deficiency increased MNNG sensitivity (Adamson *et al.*, 2005). Activation of MAPK signaling, induced by MNNG, is shown to require MLH1, c-Abl and ATM (Kim *et al.*, 2007). Moreover, they display defective activation of the kinases Chk1 and Chk2 (Brown *et al.*, 2003; Stojic *et al.*, 2004b; Wang and Qin, 2003) and dysregulation of these kinases in response to MNNG results in defective G2 arrest in MMR-deficient cells (Adamson *et al.*, 2005). All these observations implicate MMR proteins in a signaling cascade that leads from DNA damage to cell cycle arrest and/or apoptosis. The

inability of MMR-deficient cells to activate cell cycle arrest and cell death in response to MNNG and related drugs (Goldmacher *et al.*, 1986; Kat *et al.*, 1993; Koi *et al.*, 1994b; Meikrantz *et al.*, 1998) has been termed alkylation-tolerance (Branch *et al.*, 1993).

3.1.3 Summary

Agents, inducing O⁶-methylguanine (O⁶MeG) in DNA, such as *N*-methyl-*N'*-nitro-*N*-nitrosoguanidine (MNNG) are cytotoxic and a deficiency in mismatch repair (MMR) results in lack of sensitivity to this genotoxin (termed alkylation tolerance). A number of DNA damage response proteins including c-Abl, p53 and p73 are activated by MNNG in a MMR-dependent manner, and several also require ATM/ATR kinase activity. Here, we show that ING2, a member of the inhibitor of growth (ING) family proteins is upregulated in MNNG-treated cells. We further observed that ING2 regulates the cell death response induced by this alkylator through a mechanism involving acetylation and stabilization of p73. Induction/acetylation of p53, in response to MNNG, however, proceeds in an ING2-independent manner. Inhibition of c-Abl by STI571 treatment blocked ING2 upregulation and p73 acetylation induced by MNNG. Similarly, MLH1- suppressed or mutated cells displayed defective ING2 upregulation and p73 acetylation in response to MNNG. Taken together, these results indicate that MLH1- and c-Abl-dependent upregulation of ING2 activates the cell death response to MNNG through p73 acetylation. The results further suggest that inactivation of ING2>p73 signaling pathway may contribute to alkylation tolerance observed in MMR-deficient colorectal cancer cells.

3.2 MATERIALS AND METHODS

3.2.1 Materials

MNNG and Caffeine were obtained from Sigma-Aldrich (St. Louis, MO). STI 571 [Imatinib (Gleevec)] was a gift from Novartis (Basel, Switzerland). Antibodies specific for p53 (DO-1), Caspase-3 and β -tubulin were obtained from Cell Signaling (Danvers, MA). Antibodies specific for p73 α and PARP-1 were obtained from Santa Cruz Biotechnology (Santa Cruz, CA). Antibodies specific for caspase 9, acetyl-p53 (K373/K382) and acetyl-lysine were obtained from Upstate Biotechnology (Lake Placid, NY). HRP-conjugated secondary antibodies were purchased from Novus Biologicals (Littleton, CO).

3.2.2 Cell lines

HeLa, HEK-293, U2OS and HCT116 were cultured in Dulbecco's modified Eagle's medium (DMEM) supplemented with 10% fetal bovine serum (FBS). HCT116+ch2 (H2) is an MLH-deficient derivative of HCT116 that has a portion of human chromosome 2 introduced by microcell fusion. The MMR-proficient colorectal tumor line HCT116+ch3 (H3) was created by the stable transfer of a portion of human chromosome 3, bearing a wild-type copy of the hMLH1 gene, into MLH1-deficient line HCT116 (Koi *et al.*, 1994a). HCT116+ch2 and HCT116+ch3 cells were maintained in DMEM containing 10% FBS supplemented with 400 μ g/ml of geneticin (G418) as described (Koi *et al.*, 1994a). All Cells were grown at 37°C in a humidified 5% CO₂ incubator.

3.2.3 RNA interference

Overlapping synthetic oligonucleotides corresponding to sequences specific for the human ING2 (5'- AGAGAGCACTAATTAATAG -3'), p53 (5'- GACTCCAGTGGTAATCTAC -3'), p73 α (5'- CGGACTGGAAATTGTCAATATT -3') and MLH1 (5'-GGTTCACTACTAGTAAACTG-3') transcripts were hybridized and cloned into pSIREN-RETRO-Q (Clontech, La Jolla, CA). The recombinant pSiren plasmid was co-transfected with pCL-ampho plasmid encoding the packaging viral DNA into the packaging cell line, 293T (Clontech) using Lipofectamine 2000 (Invitrogen, Carlsbad, CA). The supernatant containing the viral DNA was collected, filtered and used to infect HCT116+ch3 cells with polybrene-supplemented medium. Cells were selected by incubation with puromycin (1 μ g/ml) for 4 days and downregulation of target gene expression was confirmed by immunoblotting.

3.2.4 Immunoblotting

Immunoblotting will be performed as described in 2.2.5. Cells will be treated with indicated drugs. Treated cells, as well as untreated ones, will be harvested and extracts will be made for immunoblotting. The membrane will be probed with indicated antibody.

3.2.5 Immunoprecipitation

Briefly, $\sim 1 \times 10^6$ cells were lysed in 500 μ l of 1X lysis buffer (20 mM Tris-HCl, pH7.5 / 150 mM NaCl / 5 mM EDTA / 0.5% NP40 / 1 mM NaF / 1 mM DTT / 1 mM Na-vanadate) and clarified by centrifugation. Lysates were adjusted for equal protein content and then incubated

with 5 μ l of antibody overnight at 4°C on a rocking platform. 25 μ l of 50/50 (v/v) slurry of protein A-Sepharose beads (American Pharmacia Biotech) in PBS were added and incubation continued for another 2 hours. Immune-complexes were collected by centrifugation, washed three times in 1X lysis buffer containing 300 mM NaCl, once with 1X lysis buffer, and subsequently analyzed by SDS-PAGE and immunoblotting.

3.2.6 Transfection

Cells will be cultured into 24-well plate, with each well plated with 5x10⁵ cells, and kept in 37°C incubator for 24 hours. Cells will be transfected with constructed plasmids or with empty vector. DNA for transfection will be diluted in 50 μ l Opti-MEM I medium before Lipofectamine 2000 (Invitrogen CA) is added and mixed. After being incubated for 30 min, 100 μ l of complex will be added to each well containing cells and medium. Incubate the cells at 37°C for 24 hours before testing transgene expression.

3.2.7 Flow cytometry

Mock- (DMSO) and MNNG-treated cells were washed twice with 1X PBS, fixed by treatment with ice-cold 70% ethanol for 30 min on ice and stored at 4° C prior to analysis. For staining, cells were incubated in PBS containing 1 mg/ml RNase A, 40 μ g/ml propidium iodide (Sigma-Aldrich) for 30 min in the dark at 37° C and then analyzed by flow cytometry. For each sample, more than 3 x 10⁴ cells were counted, and the cells with a lower DNA content (sub-G1) than those of the G₀/G₁ phase were referred to as apoptotic cells. DNA histograms were analyzed using ModFit (Verity Software House, Topsham, ME) software. All flow cytometry experiments

were performed in triplicate. The paired Student's t test was used to determine the statistical significance. StatView software (Abacus Concepts, Berkeley, CA) was used. A P value of less than 0.05 represented a statistically significant difference between the values of two group means.

3.3 RESULTS

3.3.1 Dose- and time-dependent Induction of ING2 in response to MNNG treatment

ING2, a member of the inhibitor of growth (ING) family has been implicated in cellular responses induced by genotoxic agents such as etoposide and neocarzinostatin (Nagashima *et al.*, 2001b). To determine its role in alkylator-induced responses, we monitored intracellular ING2 protein levels after treatment with MNNG. Immunoblotting of the lysates formed at 0, 3, 6, 12 and 24 h after treatment with MNNG (10 μ M) showed a time-dependent increase in ING2 protein level with optimal induction at 6 h post-treatment (Figure 15A, *top panel*). MNNG-treated U2OS and HEK293 cells also showed similar increases in ING2 protein after treatment with MNNG (*middle and bottom panels*). ING2 induction by MNNG is also dose-dependent as exposure to increasing concentrations of MNNG (5, 10, 25 and 50 μ M) caused a proportionate increase in ING2 protein levels (~1.4, 2.3, 4.1, and 4.5-fold ING2 increase; Figure 15B). When the induction was assessed in the presence of methyl-guanine methyl transferase (MGMT) inhibitor, O⁶-benzylguanine (BG) that increases O⁶-methyl lesions in DNA, the level of ING2 increased further compared to MNNG alone treatment (Figure 15C). Thus, we conclude that alkylator-induced DNA damage signals ING2 protein upregulation.

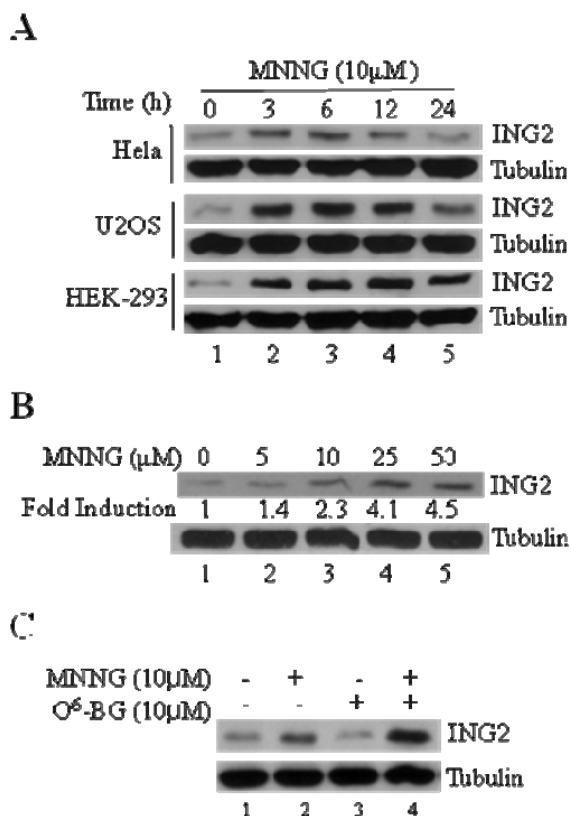


Figure 15: MNNG treatment induces ING2 in a time- and dose-dependent manner.

(A) HeLa, U2OS and 293 cells were exposed to 10 μ M MNNG and lysates were formed at 0, 3, 6 and 12 and 24 h post-treatment. Lysates were resolved on a 10% SDS-PAGE electrophoresis, transferred onto Immobilon-P and subjected to immunoblotting with rat monoclonal anti-ING2 antibody. Equal protein loading was confirmed by anti- β -tubulin antibody. (B) Dose-dependent induction of ING2 in HeLa cells. (C) MNNG-induced ING2 upregulation in HeLa cells with the presence and absence of MGMT inhibitor, O⁶-benzylguanine (10 μ M).

3.3.2 ING2 is required for MNNG-induced cell death

To examine the involvement of ING2 in cell cycle arrest/cell death responses induced by MNNG, we suppressed ING2 expression in human colorectal cancer cells (HCT116+Ch3;H3) using shRNA approaches as described in methods. As control, luciferase shRNA was used. Immunoblotting of the lysates prepared from mock- and MNNG-treated knocked down cells confirmed suppression of ING2 protein expression in shING2 cells (Figure 16A). Subsequently, shING2 and control shLuc cells were exposed to MNNG (10 μ M) and % apoptotic cell population containing sub-G1 DNA content was assessed at 12, 24, 48 and 72 h post-treatment by flow cytometry. Result showed low levels of cell death in both Luc and ING2-knocked down cells at 12 and 24 h after treatment (Figure 16B). However, at 48 and 72 h after MNNG treatment, shING2 cells showed reduced cell death compared to shLuc cells. Specifically, at 72 h after MNNG, shING2 cells showed ~2 fold reduced cell death than shLuc (31.8% sub-G1 in shING2 and ~54.8% sub-G1 in shLuc, respectively).

Immunoblotting of the lysates with anti-caspase-3 and caspase-9 antibodies showed reduced cleavage in MNNG-treated shING2 cells compared to similarly-treated shLuc cells (Figure 16C), consistent with attenuated cell death following suppression of ING2. Conversely, shLuc and shING2 cells showed comparable G2/M population at 24 and 48 h after MNNG (Figure 16D). Taken together, these results demonstrate a requirement for ING2 in the cell death response but not for G2/M arrest induced by MNNG.

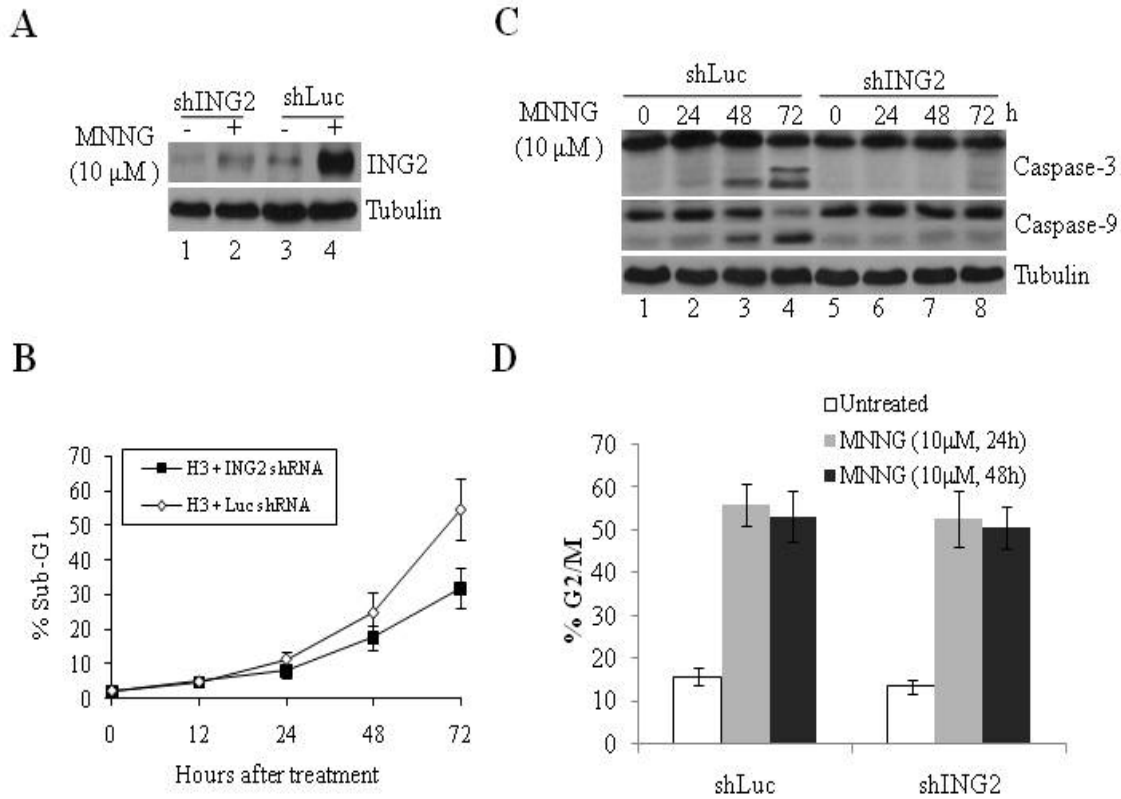


Figure 16: ING2 is required for MNNG-induced cell death.

(A) Human colorectal cancer cells (HCT116+Ch3;H3) knocked down for Luciferase (shLuc) or ING2 (shING2) were mock-treated or exposed to MNNG (10 μM) and lysates were formed 4 h later. Lysates were subjected to immunoblotting with anti-ING2 antibody. (B) MNNG (10 μM)-treated shLuc and shING2 cells were collected at 12, 24, 48 and 72 h post-treated, stained with propidium iodide and % apoptosis (sub-G1) was assessed by flow cytometry. % sub-G1 cell population obtained from at least three independent experiments with mean and *S.D* is given. (C) Cell extracts were also formed and subjected to immunoblotting with caspase-3, and caspase-9 antibodies. Equal protein content was confirmed by anti-β-tubulin antibody. (D) % G2/M cell population obtained from three independent experiments with mean and *S.D* is given.

3.3.3 ING2 is dispensable for p53 stabilization/acetylation induced by MNNG

ING2-mediated apoptosis after UV irradiation requires p53 (Chin *et al.*, 2005). To determine whether ING2-mediated cell death, induced by the alkylator (MNNG) is also dependent on p53, we monitored p53 levels in MNNG-treated shLuc and shING2. Both luciferase and ING2-knocked down cells showed similar levels of p53 induction in response to MNNG treatment (Figure 17A, *top panel*). Examination of p53 acetylation by immunoblotting with anti-acetyl p53 (K373/K382) antibody showed that p53 acetylation induced by MNNG also proceeds in an ING2-independent manner (Figure 17A, *middle panel*). We next compared cell death triggered by MNNG in cells knocked down Luc, ING2, p53 or both p53 and ING2. After confirming the suppression of protein expression by immunoblotting (Figure 17B), these cells were exposed to MNNG and cell death was assessed 72 h post-treatment. As expected, ING2-suppressed cells showed reduced cell death compared to Luc-knocked down (Figure 17C). However, cells knocked down for p53 showed only a modest reduction in cell death in response to MNNG treatment. Consistent with this result, MNNG-treated shp53 showed only a slight reduction in PARP cleavage compared to treated shLuc cells (Figure 17D; *compare lanes 6-8 to lanes 2-4*). Cells knocked down for both p53 and ING2 showed cell death attenuation similar to shING2 cells. Altogether, these results demonstrated that p53 plays a modest role in cell death induced by MNNG. Perhaps, p53 upregulation and acetylation induced by MNNG may activate its repair function.

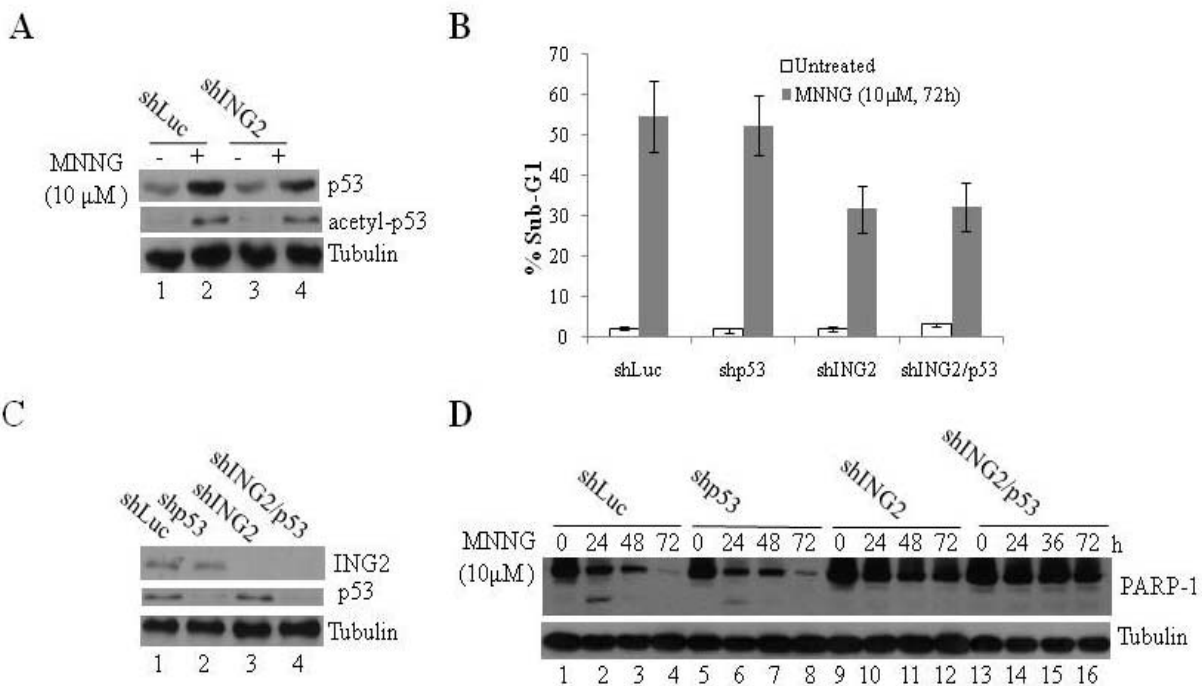


Figure 17: ING2 is dispensable for MNNG-induced p53 stabilization.

(A) Lysates formed from mock- and MNNG (10 μM)-treated shLuc and shING2 cells were subjected to immunoblotting with mouse monoclonal anti-p53 (DO-1) and anti-acetyl p53 (K372/373) antibody. Anti-β-tubulin immunoblotting shows equal protein loading. (B) shLuc, shp53, shING2 and shING2/p53 cells were exposed to MNNG (10 μM) and collected at 0 and 72 h post-treatment. Cells were stained with propidium iodide and % apoptosis (sub-G1) cells were determined by flow cytometry. Experiment was repeated three times and the mean with *S.D* is given. (C) Lysates formed from knocked down cells shown in *panel B* were subjected to immunoblotting with anti-ING2, p53 (DO-1) and tubulin antibody. (D) Lysates formed from untreated and MNNG-treated shLuc, shING2, shp53 and shING2/p53 cells were subjected to immunoblotting with anti-PARP antibody. Anti-β-tubulin immunoblotting shows equal protein loading.

3.3.4 ING2 regulates p73 induction/acetylation in response to MNNG

A recent study implicated the p53 homologue, p73 in the cell death response induced by MNNG (Li *et al.*, 2008). This prompted us to examine the requirement of ING2 in p73 α induction/acetylation induced by the alkylator. Immunoblotting of the lysates prepared from MNNG-treated shLuc and shING2 cells with anti-p73 α antibody showed modestly increased levels of p73 α at 6 and 12 h post-treatment (Figure 18A). p73 α levels in treated shING2 cells remained unchanged during these time points. We also examined p73 α acetylation by immunoprecipitation followed by immunoblotting with anti-acetyl antibody. At each of the time points examined, shLuc cells showed p73 α acetylation after treatment whereas ING2-knocked down cells showed very little acetylation. These results clearly demonstrated ING2 dependency of MNNG-induced p73 induction and acetylation. To determine if ING2 directly regulates p73 α acetylation, we overexpressed ING2 in 293T cells by transient transfection of ING2 cDNA and then examined p73 α acetylation. As shown in Figure 18B, cells transfected with ING2 cDNA showed increased p73 α acetylation compared to vector-transfected cells (*compare lane 1 and 3*). MNNG treatment further increased the cellular levels of ING2 in ING2-transfected cells (*lane 4*). We also reasoned that, perhaps ING2 interacts with p73 α to promote acetylation. To examine this possibility, we performed a co-immunoprecipitation assay. Anti-ING2 immunoprecipitates prepared from MNNG-treated 293 cells showed the presence of p73 α (Figure 18C; *top panel; lane 2*). Reprobing of the membrane with anti-acetyl antibody showed that ING2-associated p73 α is acetylated. Untreated cells showed very little interaction and acetylation of p73 α . Together, the results reinforced the notion that ING2 promotes p73 α acetylation following MNNG treatment through direct binding.

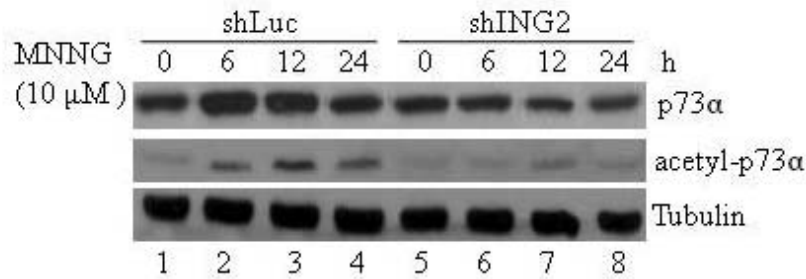
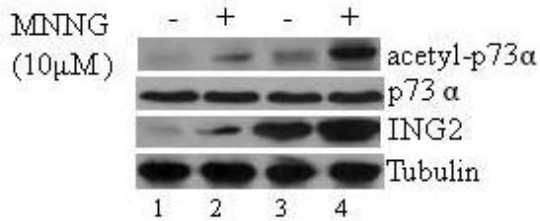
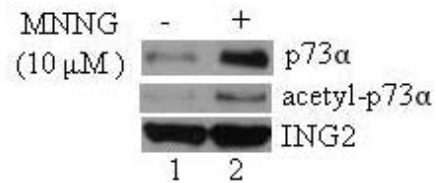
A**B****C**

Figure 18: ING2 is required for MNNG-induced p73 acetylation.

(A) ShLuc and shING2 cells were treated with MNNG (10 μM) and collected at 0, 6, 12, and 24 h later. Lysates were prepared, adjusted for equal protein concentration and then subjected to immunoblotting with anti-p73α antibody. An aliquot of the lysate was used to immunoprecipitate p73α using anti-p73α antibody. The immune-complexes were then resolved on 8% SDS-PAGE, transferred onto Immobilon-P and immunoblotted with polyclonal anti-acetyl antibody. Equal protein loading was confirmed by anti-β-tubulin immunoblotting of the lysates. (B) 293 cells transfected with vector or ING2 cDNA and then either mock-treated or exposed to MNNG (10 μM). At 4 h post-MNNG, lysates were prepared and used for assessment of p73α acetylation by immunoprecipitation followed by immunoblotting as described in *panel A*. (C) *Co-immunoprecipitation*

assay. 293 cells were exposed to MNNG (10 μ M) and lysates were prepared at 0 and 12 h after were subjected to immunoprecipitation with anti-ING2 antibody. The immune complex was resolved on 4-12% SDS-PAGE and the proteins were transferred onto Immobilon-P. The membrane was probed with anti-ING2 and anti-p73 α antibody. The membrane was stripped and then re-probed with anti-acetyl antibody.

3.3.5 p73 is required for MNNG-induced cell death.

To evaluate the functional significance of ING2-dependent p73 α induction/acetylation induced by MNNG, we compared cell death induced by this alkylator in cells suppressed either for ING2 or p73 α or both (Figure 19A). As expected, cell suppressed for ING2 showed reduced cell death compared to control luciferase knocked down cells (Figure 19B). Surprisingly, cells suppressed for p73 α showed much reduced cell death (~18.7% sub-G1) than shING2 cells (~31.8% sub-G1). Corroborating well this result, decreased Caspase-3 cleavage was observed in the MNNG-treated shp73 α cells than similarly-treated shING2 cells (Figure 19C). The comparatively reduced cell death observed in shp73 α cells than shING2 cells suggests a prominent role for p73 α in MNNG-induced apoptosis. Cells knocked down for both shING2 and p73 α cells showed cell death (~17.4% sub-G1) comparable to p73 α knocked down cells (~18.7% cell death). Caspase-3 cleavage was also comparable in shING2/p73 and shp73 α cells (Figure 19C). Clearly, although modification of p73 α induced by MNNG is dependent on ING2, the comparatively reduced cell death observed in shp73 cells than in shING2 cells suggests an ING2-independent role for p73 α in MNNG-induced cell death.

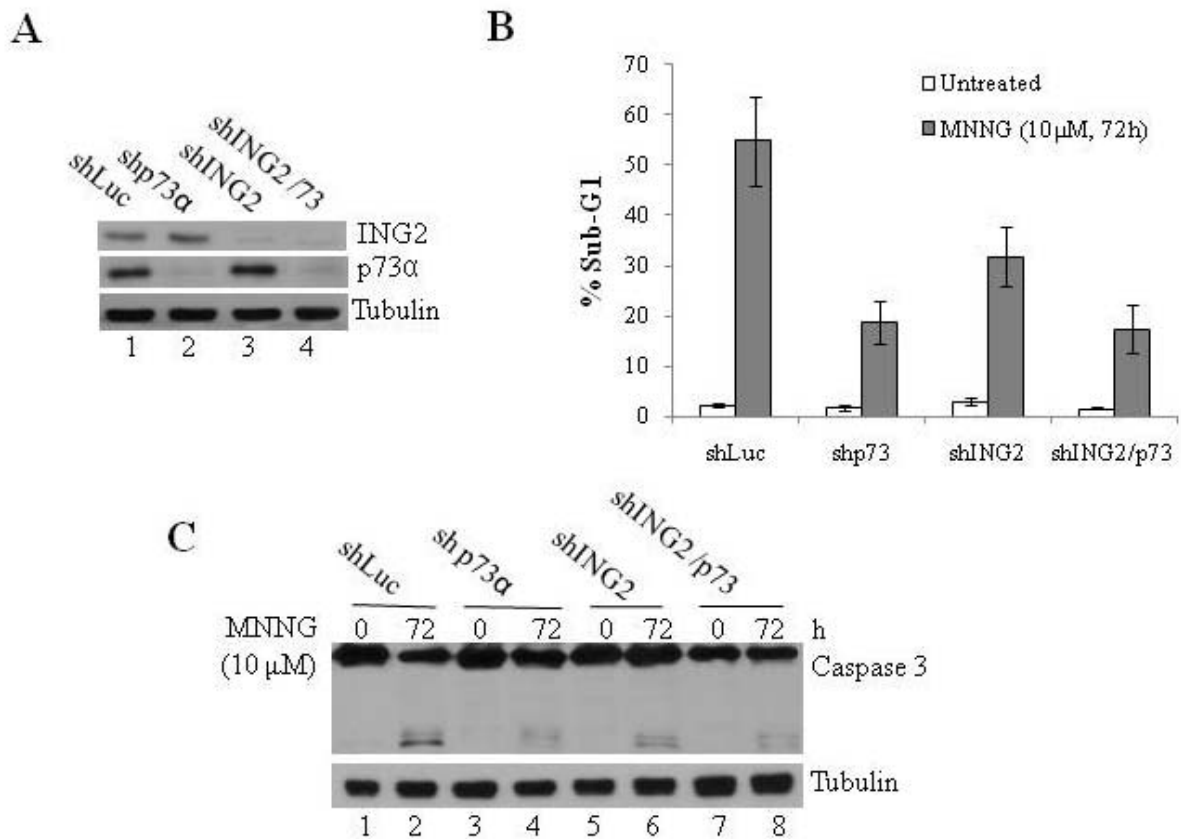


Figure 19: MNNG-induced cell death in cells knocked down for ING2, p73 or both.

(A) Lysates prepared from shLuc, shING2, shp73 and shING2/p73 cells were subjected to immunoblotting against p73 α , ING2 and tubulin antibody. (B) ShLuc, shLuc/p73, shING2 and shING2/p73 cells were mock-treated or exposed to MNNG (10 μ M) and collected at 72 h post-treatment. Cells were stained with propidium iodide and % sub-G1 cell population was assessed by flow cytometry. Mean of three experiments with S.D is given. (C) Lysates formed from mock- and MNNG-treated cells described in panel B were subjected to immunoblotting with anti-caspase-3 and anti- β -tubulin antibody.

3.3.6 C-Abl-dependent acetylation of p73 activates the cell death response to MNNG

The proto-oncogene kinase, c-Abl is activated in response to MNNG treatment (Kim *et al.*, 2007). Moreover, MNNG treatment is shown to trigger a cell death response that is dependent on c-Abl. (Li *et al.*, 2008). Given this, we asked whether Abl is required for MNNG-induced ING2 upregulation and p73 acetylation. To that end, we pretreated H3 cells with Abl inhibitor STI571 and then examined ING2 induction. As shown in Figure 20A, pretreatment with Abl inhibitor STI571, blocked ING2 upregulation (compare lane 2 to 4). In addition, STI571 blocked p73 α acetylation (Figure 20B; compare lane 2 to 4) induced by MNNG. Furthermore, STI571 treatment blocked cell death induced by MNNG, in agreement with a recent report (Li *et al.*, 2008). Clearly, c-Abl is a required component in the ING2-mediated signaling and cell death induced by MNNG.

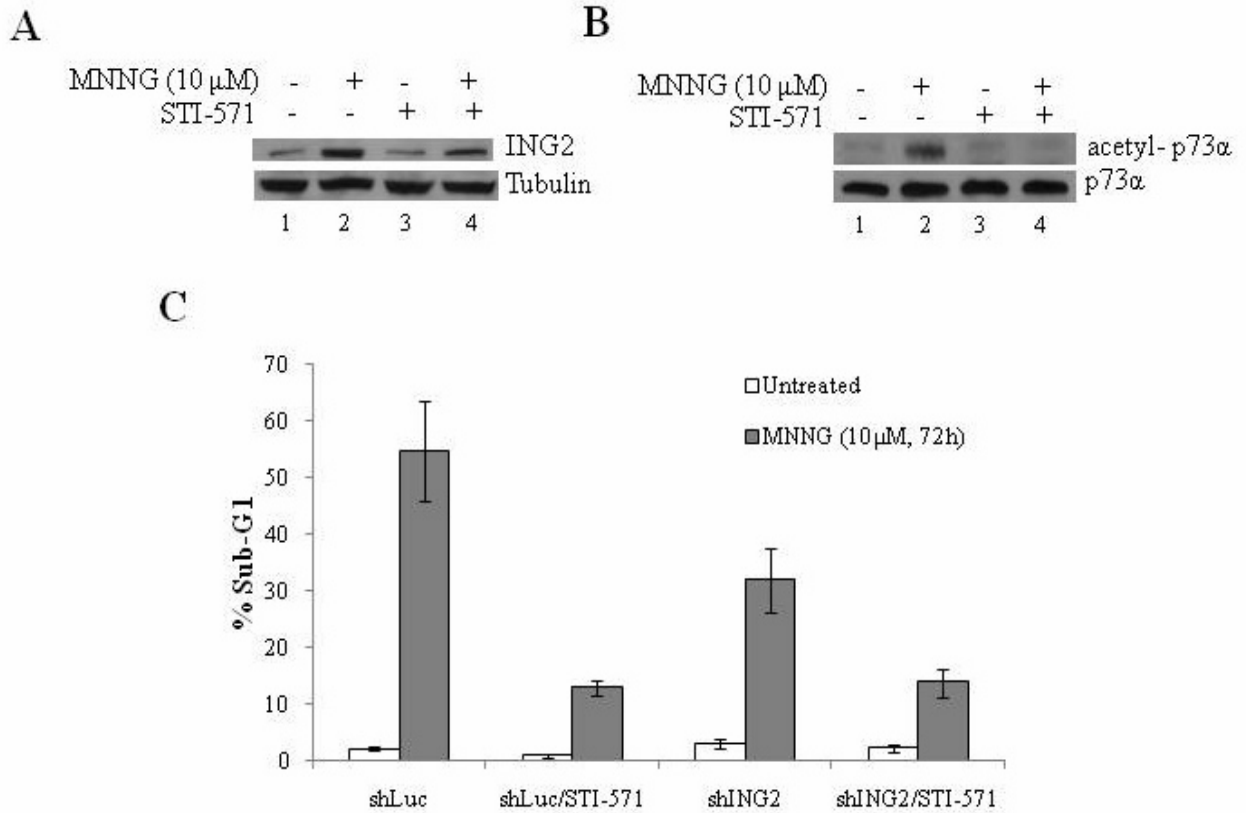


Figure 20: STI571 blocks MNNG-induced ING2 upregulation and p73 acetylation.

(A) 293 cells were exposed to MNNG (10 μ M) in the presence or absence of STI571 (1 μ M) and ING2 upregulation was assessed by immunoblotting. (B) Lysates were also used for determination of p73 acetylation status by immunoprecipitation followed by immunoblotting as described in Method. (C) shLuc and shING2 were exposed to MNNG (10 μ M) in the presence of STI571 (1 μ M) and % cell death was assessed 72 h post-MNNG by flow cytometry. Mean of three independent experiments with S.D is given.

3.3.7 MMR dependency of ING2/ p73 induction by MNNG

Since c-Abl activation by MNNG requires MMR function, we assessed its requirement in ING2/p73 α signaling induced by MNNG. To that end, we exposed MLH1-deficient (HCT116) and its isogenic-proficient (HCT116/MLH1⁺) counterpart to MNNG (10 μ M) and at varying time-points lysates were prepared and were subjected to immunoblotting with anti-ING2 antibody. As shown in Figure 21A, induction of ING2 was observed in MLH1-positive (HCT116/MLH1⁺) cells (Figure 21A; *top panel, lanes 6-8*). MLH1-deficient counterpart, on the other hand, showed very little ING2 induction (*lanes 2-4*). Assessment of p73 α induction/acetylation by immunoprecipitation followed by immunoblotting with anti-acetyl (PAN) antibody showed MMR dependency of p73 α acetylation (Figure 21A). Similarly, cells knocked down for MLH1 failed to display ING2 induction and p73 α induction/acetylation in response to MNNG treatment (Figure 21B). Together, these results demonstrated that, in addition to c-Abl, the function of MLH1 is required for activation of ING2>p73 α signaling triggered by MNNG.

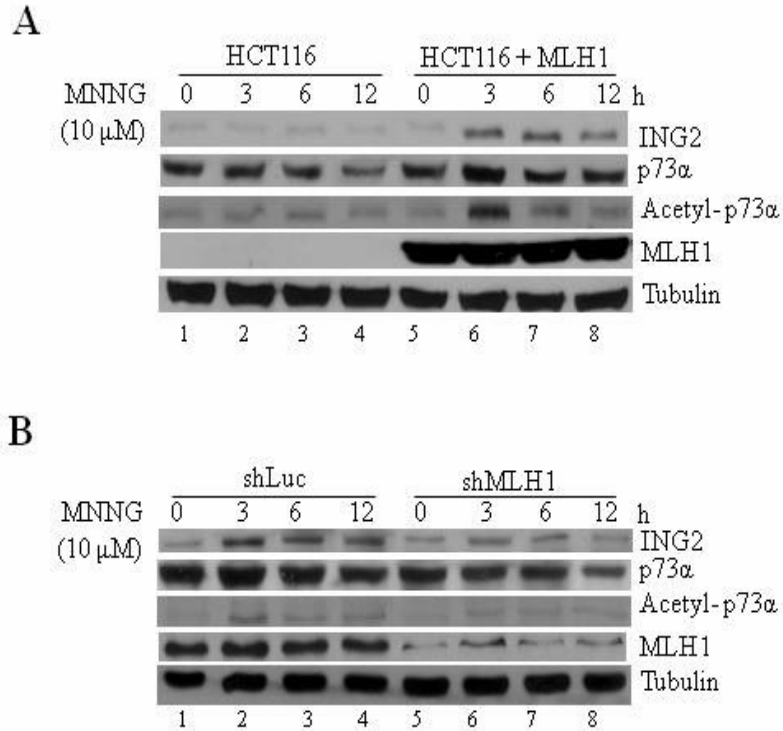


Figure 21: MMR function is required for MNNG-induced ING2 induction and p73 acetylation.

(A) MLH1-deficient (HCT116) and –proficient (HCT116/MLH1⁺) cells were exposed to MNNG (10 μ M) and lysates were formed at 0, 3, 6 and 12 h post-MNNG. Lysates were adjusted for equal protein concentration and subjected to immunoblotting with anti-ING2 antibody. The membrane was re-probed with anti-73 α antibody. An aliquot of the lysates was also subjected to immunoprecipitation with anti-p73 α antibody and the immune-complex was analyzed for acetylation status by immunoprecipitation followed by immunoblotting with anti-acetyl antibody. Anti- β -tubulin immunoblotting shows equal protein loading. (B) H3 cells knocked down for luciferase (shLuc) or MLH1 (shMLH1) were MNNG treated and at 3, 6 and 12 h post-treatment were subjected to

immunoblotting with anti-ING2, p73 α and anti-tubulin antibody. p73 α acetylation was assessed as described in *panel A*.

3.3.8 ATM/ATR independency of ING2/ p73 acetylation induction by MNNG

In addition to responding to DNA damage inflicted by IR and UV, the PI3-kinases, ATM and ATR have been shown to respond to MNNG(Adamson *et al.*, 2002). Specifically, MNNG treatment is shown to stimulate ATM/ATR kinase activity, consequently inducing a G2/M arrest response that is dependent on intact ATM/ATR function (Adamson *et al.*, 2005; Stojic *et al.*, 2004a). Given this, we asked whether ATM/ATR kinases are required for activation of ING2>p73 α signaling. For this purpose, we exposed HEK-293 cells to MNNG in the presence of ATM/ATR kinase inhibitor, caffeine and then assessed ING2 induction and p73 α acetylation. Result showed comparable ING2 upregulation in the presence or absence of caffeine (Figure 22A). We next compared normal (GM02530) and ATM-deficient human fibroblasts (GM1588A) for ING2 induction. Again, comparable ING2 accumulation was observed in MNNG-treated ATM-proficient and –deficient cells (Figure 22B). Similarly, ATM- reconstituted (YZ-5) and ATM-deficient (EBS) cells showed similar levels of ING2 accumulation in response to MNNG treatment (Figure 22C). Collectively all these results showed that the function of ATM/ATR kinases are dispensable for MNNG-induced ING2-upregulation.

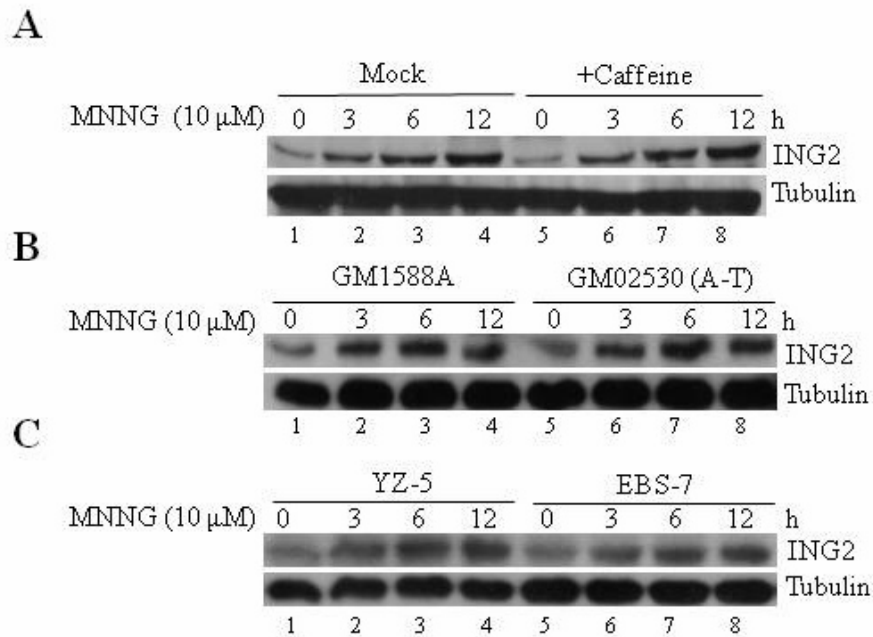


Figure 22: ATM and ATR are dispensable for MNNG-induced ING2 induction.

(A) Effect of caffeine in MNNG-induced ING2 upregulation. 293 cells were treated with caffeine (1 mM) for 1 h and then exposed to MNNG (10 μ M). Lysates were formed at 0, 3, 6 and 12 h post-MNNG and were subjected to immunoblotting with anti-ING2 antibody. Anti-tubulin immunoblotting shows equal protein loading. (B) ING2 induction in MNNG-induced ING2 induction in ATM-deficient (GM1588A) and ATM-proficient (GM02350) human fibroblasts there were treated with 10 μ M MNNG for 0, 3, 6 and 12 h. (C) ING2 upregulation following mock- and MNNG-treatment of ATM-reconstituted (YZ-5) and ATM-deficient cells.

3.4 DISCUSSION

Members of the ING family have been implicated in cellular responses triggered by IR, UV and etoposide; however, their involvement in alkylator-induced responses is not known. The work outlined in this study document an ING2-mediated signaling pathway that is activated by SN1-methylating compound, MNNG. Activation of this pathway leads to the rapid upregulation of ING2 protein that in turn, promotes cell death through acetylation and activation of proapoptotic function of p73 α . Consistent with this, suppression of ING2 protein expression by shRNA attenuated p73 α acetylation/stabilization and cell death induced by MNNG. Intact p53 acetylation/stabilization induced by MNNG in ING2-knocked down cells showed ING2 independency. The relatively modest effect of p53 suppression on MNNG-induced cell death demonstrates its dispensability in the alkylator-induced cell death. On the other hand, the greater impact of p73 α suppression on MNNG-induced cell death highlights the significance of this p53 homologue in eliciting cell death response induced by this alkylator. Since MGMT inhibitor, O⁶-Benzylguanine, that increases the O⁶MeG lesion, augments ING2 upregulation induced by MNNG, we further conclude that DNA damage is a signal for activation of ING2>p73 α activation.

3.4.1 ING2 induction and c-Abl activation

The precise molecular signaling events leading to ING2 upregulation in response to MNNG treatment are unclear. However, the lack of ING2 upregulation in MNNG-treated MMR- and Abl kinase compromised cells identified these proteins as upstream signaling elements of this pathway. It is well documented that MMR-mediated recognition and processing of O⁶-MeG

lesions lead to formation of double strand breaks. Consistent with this, several DSB responsive molecules, including ATM and Abl are activated by MNNG in MMR-dependent manner. Since ING2 protein levels is upregulated by DSB-inducing agent, neocarzinostatin (Nagashima *et al.*, 2001b), we propose that DSBs arising during MMR-mediated processing of O⁶-methylguanine lesion could trigger ING2 upregulation (Figure 23). The role c-Abl is unclear but its activation by MNNG is documented (Li *et al.*, 2008). Further, we have observed that inhibition of Abl kinase by STI571 treatment blocked ING2 upregulation induced by MNNG. Thus, activated Abl stimulates ING2 upregulation. C-Abl-mediated targeting of proteins in the ubiquitin-mediated proteosome pathway has also been reported (Sionov *et al.*, 2001). Thus, it is possible that activated Abl prevents ING2 degradation consequently leading to its upregulation. In support of this, we have observed that treatment with the Ub-mediated proteosome inhibitor, MG132 raised intracellular levels of ING2 (*data not shown*). It should be noted, however, that although ING genes are rarely mutated their transcript levels, they are often suppressed due to promoter hypermethylation in many cancer cells (Gunduz *et al.*, 2008; Gunduz *et al.*, 2000; Nagashima *et al.*, 2001b). Thus, it is possible that failure to upregulate ING2 in response to MNNG may have to do with the abnormally low levels transcription in these colorectal cancer cells. Conceivably, lack of ING2 upregulation due to promoter silencing may lead to inability of these cells to activate ING2-mediated signaling events.

3.4.2 p73 and MNNG-induced apoptosis

It is well known that acetylation activates the transcriptional function of many molecules including p53 and p73 (Costanzo *et al.*, 2002b; Ivanov *et al.*, 2007). Specifically, acetylation of p53 on lysine 120 is shown to stimulate its pro-apoptotic transcriptional activity (Sykes *et al.*,

2006; Tang *et al.*, 2006). Conceivably, ING2-mediated acetylation of p73 α stimulates its pro-apoptotic activity. As a component of mSin3-HDAC1 deacetylase complex, ING1 inhibits deacetylase activity consequently inducing p53 acetylation following upregulation during DNA damage (Skowyra *et al.*, 2001). On the other hand, ING2 is shown to facilitate p300-mediated p53 acetylation through direct interaction with p300 involving the PHD domain (Pedeux *et al.*, 2005; Wang *et al.*, 2006b). These findings allow us to propose that ING2 promotes p73 α acetylation through direct interaction and recruitment to DNA damage responsive acetyltransferase, such as p300/CBP (Pedeux *et al.*, 2005). Co-immunoprecipitation assays showed the presence of ING2/p73 α complex in MNNG-treated cells. Perhaps, recruitment of ING2/p73 complex to HAT/HDAC leads to increased acetylation. Since acetylation of p73 α correlates its modest induction, it is possible that increase in p73 α protein level could contribute to its activation. Importantly, compared to ING2-knocked down cells, p73 α -suppressed cells showed much reduced cell death in response to MNNG treatment. This finding underscores the significance of p73 and its activation by mechanisms independent of ING2 as well. Clearly, additional study is required to disseminate the role of ING2-mediated acetylation of p73 α in activating the cell death response to this alkylator.

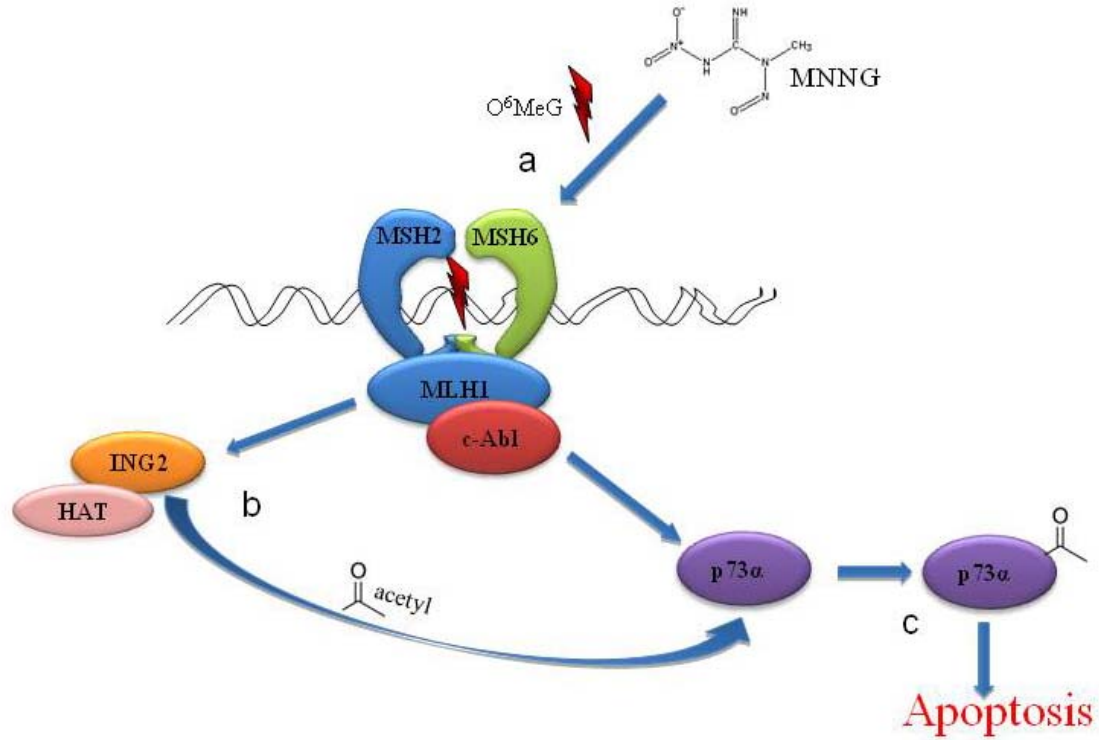


Figure 23: Proposed model for MMR-dependent activation of cell death by ING2.

a) Recognition and repair of O^6 methyl-Guanine by MMR proteins results in formation of DSB. **b)** Activation of c-Abl by DSB leads to ING2 induction which in turn promotes acetylation/stabilization of p73 α . **c)** Activated p73 α induces cell death through upregulation of apoptotic genes.

3.5 SUMMARY

In sum, the principal advance stemming from this investigation is the demonstration that a member of ING family, ING2 regulates MNNG-induced cell death through acetylation/stabilization of p73 α . The lack of ING2>p73 signaling in MMR-compromised cells suggests that inactivation of this signaling event could contribute to alkylation tolerance observed in MMR-deficient colorectal cells.

4.0 SUMMARY & FUTURE DIRECTIONS

4.1 SUMMARY

The main objective of this thesis is to elucidate the role of ING2 in mediating cellular response to DNA damage. To this end, we examined the role of ING2 in regulating responses triggered by ionizing radiation and alkylating agent. Previous studies have implicated ING2 in modulating the tumor suppressor, p53 function in response to IR through increased acetylation. However, the mechanism leading to p53 acetylation mediated by ING2 is not known. We have observed that IR activates p300 HAT activity and that the function ING2 is required for this p300 activation. Consistent with this, suppression of ING2 expression abrogated IR-induced p300 HAT activation and p53 acetylation. Additionally, we observed that protein kinase Ataxia Telangiectasia Mutated (ATM), a key regulator of IR responses is required for ING2-dependent p300 HAT activation as cells deficient in ATM displayed impaired p300 HAT activation and p53 acetylation. Restoration of ATM in A-T cells reinstated IR-induced p300 HAT activation and p53 acetylation after IR exposure. *In vitro* studies demonstrated that ING2 binds p300 in an ATM-dependent manner and that ING2 facilitates acetylation of p53 by IR-activated p300. Examination of the relationship between ATM-mediated phosphorylation and ATM-dependent acetylation of p53 revealed that phospho-p53 is a preferred target for p300 HAT. In sum, results

of our study demonstrated the convergence of ATM, p300 and ING2 in a common signaling pathway that regulates p53 function through acetylation after IR in a concerted manner.

Evaluation of the role of ING2 in alkylating agent-induced DNA damage response revealed that ING2 protein level is upregulated in response to MNNG treatment. We further observed that ING2 regulates the cell death response induced by this alkylator through a mechanism that is dependent on ING2-mediated acetylation and activation of p73 α . The function of ING2, however, was found to be dispensable for induction and acetylation of p53 triggered by MNNG. Inhibition of c-Abl kinase activity through treatment with STI571 (Gleevec) treatment blocked ING2 upregulation and p73 α acetylation induced by MNNG. Similarly, cells compromised or suppressed for MMR (MLH1) function displayed defective ING2 upregulation and p73 α acetylation. Collectively, all these results demonstrated that MMR- and c-Abl-dependent induction of ING2 regulates the cell death response to MNNG. Since O⁶-Benzylguanine (O⁶-BG) increases O⁶-methyl lesions in DNA, the level of ING2 raises further with the presence of O⁶-BG compared to MNNG alone treatment. Thus, we conclude that alkylator-induced DNA damage signals ING2 protein upregulation. Identification of p73 α as a required component in the MNNG responses established that ING2>p73 α signaling event contributes to the cell death response induced by this alkylator. The results further suggest that inactivation of ING2>p73 α signaling event may contribute to alkylation tolerance observed in MMR-deficient human colorectal cancer cells.

4.2 FUTURE DIRECTIONS

4.2.1 Mapping of ATM phosphorylation site using MALDI-TOF Mass Spectrometry

As mentioned above, a plausible explanation for ATM dependency of p300 HAT activation is that direct phosphorylation of p300 by ATM leads to increased HAT activity. ATM substrates share a common motif: X-X-X-B-(S/T)-Gln-X-X-X-X, where B can be Ala, Ile, Leu, Met, Asn, Pro, Ser, Thr or Val and X can be Cys, Arg, Lys or His (Kim *et al.*, 1999b; Manke *et al.*, 2003). We scanned the whole sequence of p300 and found 15 sites that comply with the general consensus of ATM substrate motif (Table 1). Clearly, p300 is a potential target of phosphorylation by ATM. To that end, we probed p300 immunopurified with an antibody that detects the proteins carrying phospho-(Ser/Thr) Gln motif. However, the results showed very little reactivity. Because this antibody recognizes SQ/TQ motif preceded by leucine and similar hydrophobic amino acids but not when flanked by polarized residue like glutamine, we are unable to rule out the possibility that p300 is an ATM substrate. Thus, to identify modification of p300 by phosphorylation we propose comparative mass spectrometry analysis of p300 immunopurified from normal and ATM-deficient cells.

Table 1: Candidate ATM target sequences in p300

Candidate Site	Sequence
S106	PGQVMA S QAQQSSP
T148	GPNQGP T QSTGMMN
S457	PNLSTV S QIDPSSI
T482	QVNQMP T QPQVQAK
S772	PQTQFP S QGMNVTN
S792	SGQAPV S QAQMSSS
T891	TPTPPT T QLPQQVQ
S941	QPATPL S QPAVSIE
T991	QPEPAD T QPEDISE
T1035	QPSTSAT T QSSPAPG
T1724	NQQAAAT T QSPGDSR
S1873	QTPQPT S QPQPTPP
S2047	LKPGTV S QQALQNL
S2374	DQNSML S QLASNPG
S2407	DLNSNLS S QSTLDIH

The high-accuracy matrix assisted laser desorption/ionization time-of-flight and nanoelectrospray ionization tandem mass spectrometric analysis offers an additional tool to identify potential phosphorylation site in p300. Normal and A-T cells transfected with Flag-tagged p300 could be exposed to IR and p300 enriched by binding to Flag-beads. The anti-p300 immunocomplex could be resolved on SDS-PAGE gel. The ~p300 kDa band containing excised, phosphorylated and digested products will be subjected to mass spectrophotometric analysis. A comparison of the results obtained from irradiated normal and A-T cells could potentially demonstrate whether p300 indeed is a direct phosphorylation target of ATM.

An alternate approach is that if p300 is phosphorylated by ATM and this modification upregulated p300 HAT activity then mutation of S/T site should abolish activation. Each of the 15 phosphorylation sites could be mutated and tested for abolishment of p300 HAT activation.

4.2.2 Mechanism of ING2-mediated activation of p300

The presence of PHD domains in both ING2 and p300 raises the possibility that p300 HAT activation could potentially be mediated by PHD-PHD interaction. We had speculated that interaction may allow switching the more closed configuration of p300 to an open one, resulting in accessibility of critical residues which may otherwise be buried inside. To test this, we propose to delete PHD domain in p300 and ING2 and examine interaction and activation. We documented that suppression of ING2 expression abrogated p300 activation by IR. Future study could involve creation of an internally PHD deletion mutant of ING2 and then examination of activation of p300 activity following overexpression in 293 cells. *In vitro* HAT assays employing ΔPHD ING2 could further test the proposed mechanism of p300 activation.

4.2.3 Role of ING2 relocation in p300 HAT activation

Although ING2 intracellular level is not upregulated post IR, the irradiation treatment affects the subcellular redistribution of ING2. Specifically, after irradiation, ING2 relocates from the cytoplasm to the nucleus suggesting a probable cytoplasmic and nuclear function. The requirement for ING2 re-localization in p300 HAT activation could be tested by deletion of nuclear localization signal and then examining its effect on p300 activation. Compared with control luciferase shRNA cells, ING2-knocked down cells exhibit low p53 acetylation following IR. Thus, acetylation of p53 in cells expressing the NLS deletion mutant of ING2 could be evaluated to further reinforce the notion that ING2 entry into the nucleus is a required event in the activation of p300 HAT activity and p53 acetylation.

4.2.4 ING2 induction in response to MNNG

In our study, we demonstrated the protein level of ING2 increased after MNNG treatment. Despite this, the molecular events leading to the induction remains obscure. This induction can be the result of increased transcription, enhanced translation or impaired degradation of ING2. The fact that treatment with the ubiquitin-mediated proteasome inhibitor MG132 raised the cellular levels of ING2 suggests that ING2 induction is regulated through inhibition of its degradation. This should be further explored. The induction of ING2 partly depends on functional c-Abl, whose kinase activity can be activated by MNNG (Kim *et al.*, 2007). The phosphorylation of ING2 by c-Abl could stabilize the protein or prevent ING2 from being labeled to proteasomal degradation by ubiquitin ligases. To test the hypothesis that ING2 is phosphorylated and stabilized in response to MNNG, *in vitro* kinase assay of ING2 and c-Abl

should be conducted. If the phosphorylation sites could be mapped then mutant ING2 without phosphorylation sites should be introduced into the cells and ING2 induction could be examined.

4.2.5 Role of MMR in MNNG-induced ING2 expression

We observed that ING2 upregulation after MNNG requires MMR function. Specifically, we showed that functional MLH1 is indispensable. It should be noted that MMR is composed of 6 proteins including MSH2, MSH6, PMS1, MLH1 etc. It would be interesting to see if each of these proteins is required for ING2 induction as this would establish the requirement of MMR repair complex as a whole for initiation of DNA damage signal necessary for ING2 induction. The recruitment of ING2 to the O⁶-MeG lesion also needs to be evaluated. Results of these studies will clarify the proposed model that methylation lesion triggers formation of MMR complex and this initiates the signal for ING2 upregulation.

4.2.6 ING2, p300 HAT activation and p73 acetylation in response to MNNG

ING2 intracellular level is upregulated by MNNG, while IR fails to induce ING2 expression but activates its association with histone acetyltransferase p300. There is no direct evidence that ING2 induction following MNNG treatment activates p300 HAT activity. But the acetylation of p300 acetyltransferase substrate p73 (Costanzo *et al.*, 2002a; Mantovani *et al.*, 2004) suggests that p300 may be the enzyme that acetylates p73 in response to the DNA damage inflicted by MNNG. ING2 was capable of associating with p300 and activating p300 HAT activity in regulating replicative senescence (Pedeux *et al.*, 2005). It was also reported that p300 acetylates p73 after apoptotic dose of DNA damage agent doxorubicin (Costanzo *et al.*, 2002a).

These modifications upregulate p73 transcription activity to induce pro-apoptotic gene p53AIP1. Similarly in our study, we have showed that p73 is acetylated in a time-dependent manner in response to another kind of DNA damage agent MNNG. And that acetylation correlates to the apoptosis following MNNG treatment. These findings prompted us to examine the interaction between p300 and p73 in response to MNNG and it is natural to hypothesize that MNNG-induced ING2 increases its interactions with p300, and activates its HAT activity, which results in p73 acetylation.

Unfortunately, we failed to get positive result showing direct interaction between p300 and p73 after the treatment with MNNG, but it is still possible that p300 acetylates p73 to activate p73 function of mediating cell death. To examine the hypothesis, p73 acetylation following MNNG treatment would be measured in the cells with p300 knocked out or knocked down. p73 acetylation and cell death following MNNG would also be examined in the presence or absence of p300 HAT activity inhibitor, Lys-CoA. Study of p73 acetylation in p300 knocked down cells is undergoing.

Additionally, mapping the acetylation sites of p73 is also quite worth investigating. As describe in **4.2.1**, MALDI-TOF Mass Spectrometry could be utilized to determine the acetylation sites of p73. Briefly, cells will be transfected with plasmid encoding Flag-labeled p73. MNNG treated cells will be harvested and p73 will be immunoprecipitated from the lysates. The ~73 kDa band will be the cut from the SDS-PAGE in which the immunocomplex is solved, and will be subjected to digestion and mass spectrometry analysis.

APPENDIX A. ACKNOWLEDGEMENTS

We thank Dr. Or Gozani at Stanford University for rat ING2 antibody and Dr. Curtis Harris at NIH for ING2 cDNA. This work was supported by NIH grant (GM60945) and ACS (RPG 02-031-01) to R.B.

APPENDIX B. PUBLICATIONS

1. **Sun G**, Jiang Z, Baskaran R. MMR- and c-Abl-dependent induction of ING2 regulates p73-mediated cell death response to *N*-methyl-*N'*-nitro-*N*-nitrosoguanidine (*submitted*)
2. **Sun G**, Baskaran R. ATM/ING2-dependent activation of p300 HAT activity in response to ionizing radiation (*in preparation*)
3. Jiang Z, **Sun G**, Yalowich JC, Baskaran R. DNA mismatch repair protects cells from curcumin toxicity through generation of double-strand breaks and activation of G2/M checkpoint (*in Press*)
4. Kamath R, Jiang Z, **Sun G**, Yalowich JC, Baskaran R. c-Abl kinase regulates curcumin-induced cell death through activation of c-Jun N-terminal kinase. *Mol. Pharmacol.* 2007, 71, 61-72

BIBLIOGRAPHY

Aasland R, Gibson TJ, Stewart AF (1995). The PHD finger: implications for chromatin-mediated transcriptional regulation. *Trends Biochem Sci* **20**: 56-9.

Adamson AW, Beardsley DI, Kim WJ, Gao Y, Baskaran R, Brown KD (2005). Methylator-induced, mismatch repair-dependent G2 arrest is activated through Chk1 and Chk2. *Mol Biol Cell* **16**: 1513-26.

Adamson AW, Kim WJ, Shangary S, Baskaran R, Brown KD (2002). ATM is activated in response to N-methyl-N'-nitro-N-nitrosoguanidine-induced DNA alkylation. *Journal of Biological Chemistry* **277**: 38222-9.

Avantaggiati ML, Ogryzko V, Gardner K, Giordano A, Levine AS, Kelly K (1997). Recruitment of p300/CBP in p53-dependent signal pathways. *Cell* **89**: 1175-84.

Bakkenist CJ, Kastan MB (2003). DNA damage activates ATM through intermolecular autophosphorylation and dimer dissociation.[see comment]. *Nature* **421**: 499-506.

Bandyopadhyay D, Okan NA, Bales E, Nascimento L, Cole PA, Medrano EE (2002). Down-regulation of p300/CBP histone acetyltransferase activates a senescence checkpoint in human melanocytes. *Cancer Research* **62**: 6231-9.

Banin S, Moyal L, Shieh S, Taya Y, Anderson CW, Chessa L *et al* (1998). Enhanced phosphorylation of p53 by ATM in response to DNA damage. *Science* **281**: 1674-7.

Bannister AJ, Kouzarides T (1996). The CBP co-activator is a histone acetyltransferase. *Nature* **384**: 641-3.

Baskaran R, Wood LD, Whitaker LL, Canman CE, Morgan SE, Xu Y *et al* (1997). Ataxia telangiectasia mutant protein activates c-Abl tyrosine kinase in response to ionizing radiation.[see comment]. *Nature* **387**: 516-9.

Beamish H, Lavin MF (1994). Radiosensitivity in ataxia-telangiectasia: anomalies in radiation-induced cell cycle delay. *Int J Radiat Biol* **65**: 175-84.

Bobola MS, Berger MS, Silber JR (1995). Contribution of O6-methylguanine-DNA methyltransferase to resistance to 1,3-(2-chloroethyl)-1-nitrosourea in human brain tumor-derived cell lines. *Mol Carcinog* **13**: 81-8.

Branch P, Aquilina G, Bignami M, Karran P (1993). Defective mismatch binding and a mutator phenotype in cells tolerant to DNA damage. *Nature* **362**: 652-4.

Bratton MR, Frigo DE, Vigh-Conrad KA, Fan D, Wadsworth S, McLachlan JA *et al* (2009). Organochlorine-mediated potentiation of the general coactivator p300 through p38 mitogen-activated protein kinase. *Carcinogenesis* **30**: 106-13.

Brown KD, Rathi A, Kamath R, Beardsley DI, Zhan Q, Mannino JL *et al* (2003). The mismatch repair system is required for S-phase checkpoint activation. *Nat Genet* **33**: 80-4.

Browner WS, Kahn AJ, Ziv E, Reiner AP, Oshima J, Cawthon RM *et al* (2004). The genetics of human longevity. *Am J Med* **117**: 851-60.

Budman J, Chu G (2005). Processing of DNA for nonhomologous end-joining by cell-free extract. *EMBO J* **24**: 849-60.

Cadet J, Douki T, Ravanat JL (2008). Oxidatively generated damage to the guanine moiety of DNA: mechanistic aspects and formation in cells. *Acc Chem Res* **41**: 1075-83.

Campos EI, Chin MY, Kuo WH, Li G (2004). Biological functions of the ING family tumor suppressors. *Cellular & Molecular Life Sciences* **61**: 2597-613.

Canman CE, Lim DS, Cimprich KA, Taya Y, Tamai K, Sakaguchi K *et al* (1998). Activation of the ATM kinase by ionizing radiation and phosphorylation of p53. *Science* **281**: 1677-9.

Chehab NH, Malikzay A, Appel M, Halazonetis TD (2000). Chk2/hCds1 functions as a DNA damage checkpoint in G(1) by stabilizing p53. *Genes Dev* **14**: 278-88.

Chin MY, Ng KC, Li G (2005). The novel tumor suppressor p33ING2 enhances UVB-induced apoptosis in human melanoma cells. *Exp Cell Res* **304**: 531-43.

Costanzo A, Merlo P, Pediconi N, Fulco M, Sartorelli V, Cole PA *et al* (2002a). DNA damage-dependent acetylation of p73 dictates the selective activation of apoptotic target genes. *Molecular Cell* **9**: 175-86.

Costanzo A, Merlo P, Pediconi N, Fulco M, Sartorelli V, Cole PA *et al* (2002b). DNA damage-dependent acetylation of p73 dictates the selective activation of apoptotic target genes. *Mol Cell* **9**: 175-86.

Di Leonardo A, Linke SP, Clarkin K, Wahl GM (1994). DNA damage triggers a prolonged p53-dependent G1 arrest and long-term induction of Cip1 in normal human fibroblasts. *Genes Dev* **8**: 2540-51.

Doyon Y, Cayrou C, Ullah M, Landry AJ, Cote V, Selleck W *et al* (2006). ING tumor suppressor proteins are critical regulators of chromatin acetylation required for genome expression and perpetuation. *Mol Cell* **21**: 51-64.

Doyon Y, Selleck W, Lane WS, Tan S, Cote J (2004). Structural and functional conservation of the NuA4 histone acetyltransferase complex from yeast to humans. *Mol Cell Biol* **24**: 1884-96.

Duckett DR, Drummond JT, Murchie AI, Reardon JT, Sancar A, Lilley DM *et al* (1996). Human MutS α recognizes damaged DNA base pairs containing O6-methylguanine, O4-methylthymine, or the cisplatin-d(GpG) adduct. *Proc Natl Acad Sci U S A* **93**: 6443-7.

Eadie JS, Conrad M, Toorchen D, Topal MD (1984). Mechanism of mutagenesis by O6-methylguanine. *Nature* **308**: 201-3.

el-Deiry WS, Tokino T, Velculescu VE, Levy DB, Parsons R, Trent JM *et al* (1993). WAF1, a potential mediator of p53 tumor suppression. *Cell* **75**: 817-25.

Falck J, Petrini JH, Williams BR, Lukas J, Bartek J (2002). The DNA damage-dependent intra-S phase checkpoint is regulated by parallel pathways. *Nat Genet* **30**: 290-4.

Foote RS, Mitra S, Pal BC (1980). Demethylation of O6-methylguanine in a synthetic DNA polymer by an inducible activity in Escherichia coli. *Biochem Biophys Res Commun* **97**: 654-9.

Gayther SA, Batley SJ, Linger L, Bannister A, Thorpe K, Chin SF *et al* (2000). Mutations truncating the EP300 acetylase in human cancers. *Nature Genetics* **24**: 300-3.

Goldmacher VS, Cuzick RA, Jr., Thilly WG (1986). Isolation and partial characterization of human cell mutants differing in sensitivity to killing and mutation by methylnitrosourea and N-methyl-N'-nitro-N-nitrosoguanidine. *J Biol Chem* **261**: 12462-71.

Gong W, Suzuki K, Russell M, Riabowol K (2005). Function of the ING family of PHD proteins in cancer. *Int J Biochem Cell Biol* **37**: 1054-65.

Gossen M, Bujard H (1992). Tight control of gene expression in mammalian cells by tetracycline-responsive promoters. *Proc Natl Acad Sci U S A* **89**: 5547-51.

Gottifredi V, Shieh S, Taya Y, Prives C (2001). p53 accumulates but is functionally impaired when DNA synthesis is blocked. *Proc Natl Acad Sci U S A* **98**: 1036-41.

Gozani O, Karuman P, Jones DR, Ivanov D, Cha J, Lugovskoy AA *et al* (2003). The PHD finger of the chromatin-associated protein ING2 functions as a nuclear phosphoinositide receptor. *Cell* **114**: 99-111.

Griffin S, Branch P, Xu YZ, Karran P (1994). DNA mismatch binding and incision at modified guanine bases by extracts of mammalian cells: implications for tolerance to DNA methylation damage. *Biochemistry* **33**: 4787-93.

Gu W, Roeder RG (1997). Activation of p53 sequence-specific DNA binding by acetylation of the p53 C-terminal domain. *Cell* **90**: 595-606.

Gunduz M, Gunduz E, Rivera RS, Nagatsuka H (2008). The inhibitor of growth (ING) gene family: potential role in cancer therapy. *Curr Cancer Drug Targets* **8**: 275-84.

Gunduz M, Ouchida M, Fukushima K, Hanafusa H, Etani T, Nishioka S *et al* (2000). Genomic structure of the human ING1 gene and tumor-specific mutations detected in head and neck squamous cell carcinomas. *Cancer Res* **60**: 3143-6.

Hartwell LH, Kastan MB (1994). Cell cycle control and cancer. *Science* **266**: 1821-8.

Hirao A, Kong YY, Matsuoka S, Wakeham A, Ruland J, Yoshida H *et al* (2000). DNA damage-induced activation of p53 by the checkpoint kinase Chk2. *Science* **287**: 1824-7.

Howe L, Kusch T, Muster N, Chaterji R, Yates JR, 3rd, Workman JL (2002). Yng1p modulates the activity of Sas3p as a component of the yeast NuA3 Hhistone acetyltransferase complex. *Mol Cell Biol* **22**: 5047-53.

Ito A, Lai CH, Zhao X, Saito S, Hamilton MH, Appella E *et al* (2001). p300/CBP-mediated p53 acetylation is commonly induced by p53-activating agents and inhibited by MDM2. *EMBO Journal* **20**: 1331-40.

Ivanov GS, Ivanova T, Kurash J, Ivanov A, Chuikov S, Gizatullin F *et al* (2007). Methylation-acetylation interplay activates p53 in response to DNA damage. *Mol Cell Biol* **27**: 6756-69.

Jacobson S, Pillus L (1999). Modifying chromatin and concepts of cancer. *Curr Opin Genet Dev* **9**: 175-84.

Jeffy BD, Hockings JK, Kemp MQ, Morgan SS, Hager JA, Beliakoff J *et al* (2005). An estrogen receptor-alpha/p300 complex activates the BRCA-1 promoter at an AP-1 site that binds Jun/Fos transcription factors: repressive effects of p53 on BRCA-1 transcription. *Neoplasia* **7**: 873-82.

Jeong J, Juhn K, Lee H, Kim SH, Min BH, Lee KM *et al* (2007). SIRT1 promotes DNA repair activity and deacetylation of Ku70. *Exp Mol Med* **39**: 8-13.

Jung D, Alt FW (2004). Unraveling V(D)J recombination; insights into gene regulation. *Cell* **116**: 299-311.

Kaina B, Christmann M, Naumann S, Roos WP (2007). MGMT: key node in the battle against genotoxicity, carcinogenicity and apoptosis induced by alkylating agents. *DNA Repair (Amst)* **6**: 1079-99.

Kalamegham R, Warmels-Rodenhiser S, MacDonald H, Ebisuzaki K (1988). O6-methylguanine-DNA methyltransferase-defective human cell mutant: O6-methylguanine, DNA strand breaks and cytotoxicity. *Carcinogenesis* **9**: 1749-53.

Kat A, Thilly WG, Fang WH, Longley MJ, Li GM, Modrich P (1993). An alkylation-tolerant, mutator human cell line is deficient in strand-specific mismatch repair. *Proc Natl Acad Sci U S A* **90**: 6424-8.

Kataoka H, Bonnefin P, Vieyra D, Feng X, Hara Y, Miura Y *et al* (2003). ING1 represses transcription by direct DNA binding and through effects on p53. *Cancer Res* **63**: 5785-92.

Kim GD, Choi YH, Dimtchev A, Jeong SJ, Dritschilo A, Jung M (1999a). Sensing of ionizing radiation-induced DNA damage by ATM through interaction with histone deacetylase. *J Biol Chem* **274**: 31127-30.

Kim ST, Lim DS, Canman CE, Kastan MB (1999b). Substrate specificities and identification of putative substrates of ATM kinase family members. *Journal of Biological Chemistry* **274**: 37538-43.

Kim WJ, Beardsley DI, Adamson AW, Brown KD (2005). The monofunctional alkylating agent N-methyl-N'-nitro-N-nitrosoguanidine triggers apoptosis through p53-dependent and -independent pathways. *Toxicol Appl Pharmacol* **202**: 84-98.

Kim WJ, Rajasekaran B, Brown KD (2007). MLH1- and ATM-dependent MAPK signaling is activated through c-Abl in response to the alkylator N-methyl-N'-nitro-N'-nitrosoguanidine. *J Biol Chem* **282**: 32021-31.

Koi M, Umar A, Chauhan DP, Cherian SP, Carethers JM, Kunkel TA *et al* (1994a). Human chromosome 3 corrects mismatch repair deficiency and microsatellite instability and reduces N-methyl-N'-nitro-N-nitrosoguanidine tolerance in colon tumor cells with homozygous hMLH1 mutation. *Cancer Res* **54**: 4308-12.

Koi M, Umar A, Chauhan DP, Cherian SP, Carethers JM, Kunkel TA *et al* (1994b). Human chromosome 3 corrects mismatch repair deficiency and microsatellite instability and reduces N-methyl-N'-nitro-N-nitrosoguanidine tolerance in colon tumor cells with homozygous hMLH1 mutation. *Cancer Res* **54**: 4308-12.

Kuzmichev A, Zhang Y, Erdjument-Bromage H, Tempst P, Reinberg D (2002). Role of the Sin3-histone deacetylase complex in growth regulation by the candidate tumor suppressor p33(ING1). *Mol Cell Biol* **22**: 835-48.

Lau OD, Kundu TK, Soccio RE, Ait-Si-Ali S, Khalil EM, Vassilev A *et al* (2000). HATs off: selective synthetic inhibitors of the histone acetyltransferases p300 and PCAF. *Molecular Cell* **5**: 589-95.

Lavin MF, Khanna KK (1999). ATM: the protein encoded by the gene mutated in the radiosensitive syndrome ataxia-telangiectasia. *Int J Radiat Biol* **75**: 1201-14.

Lavin MF, Shiloh Y (1997). The genetic defect in ataxia-telangiectasia. *Annual Review of Immunology* **15**: 177-202.

Lee JH, Paull TT (2004). Direct activation of the ATM protein kinase by the Mre11/Rad50/Nbs1 complex. *Science* **304**: 93-6.

Lee JH, Paull TT (2005). ATM activation by DNA double-strand breaks through the Mre11-Rad50-Nbs1 complex.[see comment]. *Science* **308**: 551-4.

Li GM (2008). Mechanisms and functions of DNA mismatch repair. *Cell Res* **18**: 85-98.

Li LS, Morales JC, Hwang A, Wagner MW, Boothman DA (2008). DNA mismatch repair-dependent activation of c-Abl/p73alpha/GADD45alpha-mediated apoptosis. *J Biol Chem* **283**: 21394-403.

Lim DS, Kim ST, Xu B, Maser RS, Lin J, Petrini JH *et al* (2000). ATM phosphorylates p95/nbs1 in an S-phase checkpoint pathway. *Nature* **404**: 613-7.

Lindahl T, Wood RD (1999). Quality control by DNA repair. *Science* **286**: 1897-905.

Liu L, Scolnick DM, Trievel RC, Zhang HB, Marmorstein R, Halazonetis TD *et al* (1999). p53 sites acetylated in vitro by PCAF and p300 are acetylated in vivo in response to DNA damage. *Molecular & Cellular Biology* **19**: 1202-9.

Loeb LA, Loeb KR, Anderson JP (2003). Multiple mutations and cancer. *Proc Natl Acad Sci U S A* **100**: 776-81.

Loveless A (1969). Possible relevance of O-6 alkylation of deoxyguanosine to the mutagenicity and carcinogenicity of nitrosamines and nitrosamides. *Nature* **223**: 206-7.

Manke IA, Lowery DM, Nguyen A, Yaffe MB (2003). BRCT repeats as phosphopeptide-binding modules involved in protein targeting.[see comment]. *Science* **302**: 636-9.

Mantovani F, Piazza S, Gostissa M, Strano S, Zacchi P, Mantovani R *et al* (2004). Pin1 links the activities of c-Abl and p300 in regulating p73 function. *Mol Cell* **14**: 625-36.

Martin DG, Baetz K, Shi X, Walter KL, MacDonald VE, Wlodarski MJ *et al* (2006). The Yng1p plant homeodomain finger is a methyl-histone binding module that recognizes lysine 4-methylated histone H3. *Mol Cell Biol* **26**: 7871-9.

Matsuoka S, Rotman G, Ogawa A, Shiloh Y, Tamai K, Elledge SJ (2000). Ataxia telangiectasia-mutated phosphorylates Chk2 in vivo and in vitro. *Proceedings of the National Academy of Sciences of the United States of America* **97**: 10389-94.

Maya R, Balass M, Kim ST, Shkedy D, Leal JF, Shifman O *et al* (2001). ATM-dependent phosphorylation of Mdm2 on serine 395: role in p53 activation by DNA damage. *Genes Dev* **15**: 1067-77.

Meikrantz W, Bergom MA, Memisoglu A, Samson L (1998). O6-alkylguanine DNA lesions trigger apoptosis. *Carcinogenesis* **19**: 369-72.

Meyers M, Wagner MW, Hwang HS, Kinsella TJ, Boothman DA (2001). Role of the hMLH1 DNA mismatch repair protein in fluoropyrimidine-mediated cell death and cell cycle responses. *Cancer Res* **61**: 5193-201.

Modrich P, Lahue R (1996). Mismatch repair in replication fidelity, genetic recombination, and cancer biology. *Annu Rev Biochem* **65**: 101-33.

Moore JK, Haber JE (1996). Cell cycle and genetic requirements of two pathways of nonhomologous end-joining repair of double-strand breaks in *Saccharomyces cerevisiae*. *Mol Cell Biol* **16**: 2164-73.

Nagashima M, Shiseki M, Miura K, Hagiwara K, Linke SP, Pedoux R *et al* (2001a). DNA damage-inducible gene p33ING2 negatively regulates cell proliferation through acetylation of p53. *Proceedings of the National Academy of Sciences of the United States of America* **98**: 9671-6.

Nagashima M, Shiseki M, Miura K, Hagiwara K, Linke SP, Pedoux R *et al* (2001b). DNA damage-inducible gene p33ING2 negatively regulates cell proliferation through acetylation of p53. *Proc Natl Acad Sci U S A* **98**: 9671-6.

Nourani A, Doyon Y, Utley RT, Allard S, Lane WS, Cote J (2001). Role of an ING1 growth regulator in transcriptional activation and targeted histone acetylation by the NuA4 complex. *Mol Cell Biol* **21**: 7629-40.

Nourani A, Howe L, Pray-Grant MG, Workman JL, Grant PA, Cote J (2003). Opposite role of yeast ING family members in p53-dependent transcriptional activation. *J Biol Chem* **278**: 19171-5.

Ogryzko VV, Schiltz RL, Russanova V, Howard BH, Nakatani Y (1996). The transcriptional coactivators p300 and CBP are histone acetyltransferases. *Cell* **87**: 953-9.

Olsson M, Lindahl T (1980). Repair of alkylated DNA in *Escherichia coli*. Methyl group transfer from O6-methylguanine to a protein cysteine residue. *J Biol Chem* **255**: 10569-71.

Pacini A, Quattrone A, Denegri M, Fiorillo C, Nediani C, Ramon y Cajal S *et al* (1999). Transcriptional down-regulation of poly(ADP-ribose) polymerase gene expression by E1A

binding to pRb proteins protects murine keratinocytes from radiation-induced apoptosis. *J Biol Chem* **274**: 35107-12.

Pedeux R, Sengupta S, Shen JC, Demidov ON, Saito S, Onogi H *et al* (2005). ING2 regulates the onset of replicative senescence by induction of p300-dependent p53 acetylation. *Mol Cell Biol* **25**: 6639-48.

Pena PV, Davrazou F, Shi X, Walter KL, Verkhusha VV, Gozani O *et al* (2006). Molecular mechanism of histone H3K4me3 recognition by plant homeodomain of ING2. *Nature* **442**: 100-3.

Peng CY, Graves PR, Thoma RS, Wu Z, Shaw AS, Piwnicka-Worms H (1997). Mitotic and G2 checkpoint control: regulation of 14-3-3 protein binding by phosphorylation of Cdc25C on serine-216. *Science* **277**: 1501-5.

Petrij F, Giles RH, Dauwerse HG, Saris JJ, Hennekam RC, Masuno M *et al* (1995). Rubinstein-Taybi syndrome caused by mutations in the transcriptional co-activator CBP. *Nature* **376**: 348-51.

Pietsch EC, Sykes SM, McMahon SB, Murphy ME (2008). The p53 family and programmed cell death. *Oncogene* **27**: 6507-21.

Puri PL, Avantaggiati ML, Balsano C, Sang N, Graessmann A, Giordano A *et al* (1997). p300 is required for MyoD-dependent cell cycle arrest and muscle-specific gene transcription. *EMBO J* **16**: 369-83.

Rapic-Otrin V, McLenigan MP, Bisi DC, Gonzalez M, Levine AS (2002). Sequential binding of UV DNA damage binding factor and degradation of the p48 subunit as early events after UV irradiation. *Nucleic Acids Res* **30**: 2588-98.

Roos WP, Batista LF, Naumann SC, Wick W, Weller M, Menck CF *et al* (2007). Apoptosis in malignant glioma cells triggered by the temozolomide-induced DNA lesion O6-methylguanine. *Oncogene* **26**: 186-97.

Saito S, Goodarzi AA, Higashimoto Y, Noda Y, Lees-Miller SP, Appella E *et al* (2002). ATM mediates phosphorylation at multiple p53 sites, including Ser(46), in response to ionizing radiation. *J Biol Chem* **277**: 12491-4.

Sakaguchi K, Herrera JE, Saito S, Miki T, Bustin M, Vassilev A *et al* (1998). DNA damage activates p53 through a phosphorylation-acetylation cascade. *Genes & Development* **12**: 2831-41.

Savitsky K, Bar-Shira A, Gilad S, Rotman G, Ziv Y, Vanagaite L *et al* (1995). A single ataxia telangiectasia gene with a product similar to PI-3 kinase.[see comment]. *Science* **268**: 1749-53.

Shangary S, Brown KD, Adamson AW, Edmonson S, Ng B, Pandita TK *et al* (2000). Regulation of DNA-dependent protein kinase activity by ionizing radiation-activated abl kinase is an ATM-dependent process. *Journal of Biological Chemistry* **275**: 30163-8.

Shi X, Hong T, Walter KL, Ewalt M, Michishita E, Hung T *et al* (2006). ING2 PHD domain links histone H3 lysine 4 methylation to active gene repression. *Nature* **442**: 96-9.

Shieh SY, Ikeda M, Taya Y, Prives C (1997). DNA damage-induced phosphorylation of p53 alleviates inhibition by MDM2. *Cell* **91**: 325-34.

Shiloh Y (2003). ATM and related protein kinases: safeguarding genome integrity. *Nat Rev Cancer* **3**: 155-68.

Shimada Y, Saito A, Suzuki M, Takahashi E, Horie M (1998). Cloning of a novel gene (ING1L) homologous to ING1, a candidate tumor suppressor. *Cytogenetics & Cell Genetics* **83**: 232-5.

Sionov RV, Coen S, Goldberg Z, Berger M, Bercovich B, Ben-Neriah Y *et al* (2001). c-Abl regulates p53 levels under normal and stress conditions by preventing its nuclear export and ubiquitination. *Mol Cell Biol* **21**: 5869-78.

Skowrya D, Zeremski M, Neznanov N, Li M, Choi Y, Uesugi M *et al* (2001). Differential association of products of alternative transcripts of the candidate tumor suppressor ING1 with the mSin3/HDAC1 transcriptional corepressor complex. *J Biol Chem* **276**: 8734-9.

Stadtman ER (1992). Protein oxidation and aging. *Science* **257**: 1220-4.

Stojic L, Brun R, Jiricny J (2004a). Mismatch repair and DNA damage signalling. *DNA Repair (Amst)* **3**: 1091-101.

Stojic L, Mojas N, Cejka P, Di Pietro M, Ferrari S, Marra G *et al* (2004b). Mismatch repair-dependent G2 checkpoint induced by low doses of SN1 type methylating agents requires the ATR kinase. *Genes Dev* **18**: 1331-44.

Sykes SM, Mellert HS, Holbert MA, Li K, Marmorstein R, Lane WS *et al* (2006). Acetylation of the p53 DNA-binding domain regulates apoptosis induction. *Mol Cell* **24**: 841-51.

Tanaka Y, Naruse I, Maekawa T, Masuya H, Shiroishi T, Ishii S (1997). Abnormal skeletal patterning in embryos lacking a single Cbp allele: a partial similarity with Rubinstein-Taybi syndrome. *Proc Natl Acad Sci U S A* **94**: 10215-20.

Tang Y, Luo J, Zhang W, Gu W (2006). Tip60-dependent acetylation of p53 modulates the decision between cell-cycle arrest and apoptosis. *Mol Cell* **24**: 827-39.

Tominaga Y, Tsuzuki T, Shiraishi A, Kawate H, Sekiguchi M (1997). Alkylation-induced apoptosis of embryonic stem cells in which the gene for DNA-repair, methyltransferase, had been disrupted by gene targeting. *Carcinogenesis* **18**: 889-96.

Unger T, Juven-Gershon T, Moallem E, Berger M, Vogt Sionov R, Lozano G *et al* (1999). Critical role for Ser20 of human p53 in the negative regulation of p53 by Mdm2. *EMBO Journal* **18**: 1805-14.

van Gent DC, Hoeijmakers JH, Kanaar R (2001). Chromosomal stability and the DNA double-stranded break connection. *Nature Reviews Genetics* **2**: 196-206.

Vessey CJ, Norbury CJ, Hickson ID (1999). Genetic disorders associated with cancer predisposition and genomic instability. *Progress in Nucleic Acid Research & Molecular Biology* **63**: 189-221.

Vieyra D, Loewith R, Scott M, Bonnefin P, Boisvert FM, Cheema P *et al* (2002). Human ING1 proteins differentially regulate histone acetylation. *J Biol Chem* **277**: 29832-9.

Wang J, Chin MY, Li G (2006a). The novel tumor suppressor p33ING2 enhances nucleotide excision repair via inducement of histone H4 acetylation and chromatin relaxation. *Cancer Res* **66**: 1906-11.

Wang Y, Qin J (2003). MSH2 and ATR form a signaling module and regulate two branches of the damage response to DNA methylation. *Proc Natl Acad Sci U S A* **100**: 15387-92.

Wang Y, Wang J, Li G (2006b). Leucine zipper-like domain is required for tumor suppressor ING2-mediated nucleotide excision repair and apoptosis. *FEBS Lett* **580**: 3787-93.

Wyatt MD, Pittman DL (2006). Methylating agents and DNA repair responses: Methylated bases and sources of strand breaks. *Chem Res Toxicol* **19**: 1580-94.

Xu B, Kim ST, Lim DS, Kastan MB (2002). Two molecularly distinct G(2)/M checkpoints are induced by ionizing irradiation. *Mol Cell Biol* **22**: 1049-59.

Yao TP, Oh SP, Fuchs M, Zhou ND, Ch'ng LE, Newsome D *et al* (1998). Gene dosage-dependent embryonic development and proliferation defects in mice lacking the transcriptional integrator p300. *Cell* **93**: 361-72.

Yoshida K (2007). Regulation for nuclear targeting of the Abl tyrosine kinase in response to DNA damage. *Adv Exp Med Biol* **604**: 155-65.

Yoshida K (2008). Nuclear trafficking of pro-apoptotic kinases in response to DNA damage. *Trends Mol Med* **14**: 305-13.

Yuan W, Condorelli G, Caruso M, Felsani A, Giordano A (1996). Human p300 protein is a coactivator for the transcription factor MyoD. *J Biol Chem* **271**: 9009-13.

Yuan ZM, Huang Y, Ishiko T, Nakada S, Utsugisawa T, Shioya H *et al* (1999). Function for p300 and not CBP in the apoptotic response to DNA damage. *Oncogene* **18**: 5714-7.

Zeng X, Li X, Miller A, Yuan Z, Yuan W, Kwok RP *et al* (2000). The N-terminal domain of p73 interacts with the CH1 domain of p300/CREB binding protein and mediates transcriptional activation and apoptosis. *Molecular & Cellular Biology* **20**: 1299-310.

Zhong Q, Boyer TG, Chen PL, Lee WH (2002). Deficient nonhomologous end-joining activity in cell-free extracts from Brcal-null fibroblasts. *Cancer Res* **62**: 3966-70.

Ziv Y, Bar-Shira A, Pecker I, Russell P, Jorgensen TJ, Tsarfati I *et al* (1997). Recombinant ATM protein complements the cellular A-T phenotype. *Oncogene* **15**: 159-67.